Universitat Autònoma de Barcelona

EL PAPER ESTRUCTURAL DEL ZINC EN EL PLEGAMENT DE LES METAL·LOTIONEÏNES DE COURE

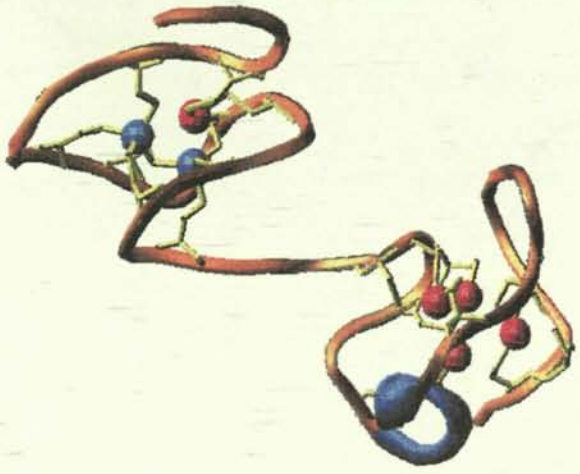

TESI DOCTORAL

Roger Bofill i Arasa

Març 2001

2. ARTICLES

Article 1

R. Bofill, O. Palacios, M. Capdevila, N. Cols, R. Gonzàlez-Duarte,

S. Atrian, P. Gonzàlez-Duarte.

A new insight into the Ag^{+} and Cu^{+} binding sites in the metallothionein β domain.

J. Inorg. Biochem., **1999**, *73*, 57-64.

ELSEVIER

Journal of Inorganic Biochemistry 73 (1999) 57–64

JOURNAL OF Inorganic Biochemistry

A new insight into the Ag^+ and Cu^+ binding sites in the metallothionein β domain

Roger Bofill [a], Òscar Palacios [a], Mercè Capdevila [a], Neus Cols [b],, Roser González-Duarte [b], Sílvia Atrian [b], Pilar González-Duarte [a,*]

[a] *Departament de Química Facultat de Ciencies, Universitat Autonoma de Barcelona, Bellaterra, E 08193 Barcelona Spain*
[b] *Departament de Genetica Facultat de Biologia Universitat de Barcelona, Avinguda Diagonal 645, E 08071 Barcelona, Spain*

Received 23 July 1998, received in revised form 23 October 1998, accepted 16 November 1998

Abstract

The copper(I) and silver(I) binding properties of the β fragment of recombinant mouse metallothionein 1 have been studied by electronic absorption and circular dichroism spectroscopy When possible, the stoichiometry of the species formed was confirmed by electrospray mass spectrometry The behaviour observed differs from that reported for the native protein Titration of either Zn_3-βMT at pH 7 or apo βMT at pH 3 with Cu^+ leads to the formation of species having the same stoichiometry and structure Cu_6-βMT, Cu_7-βMT and Cu_{10}-βMT In the first stage of the titration of Zn_3-βMT with Cu^+ at pH 7 one additional species of formula Cu_4Zn_1-βMT was detected In contrast, the titration of Zn_3-βMT at pH 7 5 and of apo-βMT at pH 2 5 with Ag^+ proceeds through different reaction pathways, affording Zn_xAg_3-βMT, Ag_6-βMT and Ag_9-βMT or Ag_3-βMT, Ag_6-βMT and Ag_9-βMT, respectively The CD envelope corresponding to species with the same stoichiometric ratio, Ag_6-βMT and Ag_9-βMT, indicates that they have a different structure at each pH value On the basis of the differences observed, the postulated similarity between copper and silver binding to metallothionein may be questioned

Keywords Recombinant β metallothionein, Metallothionein, Copper(I) binding, Silver(I) binding, β Fragment

1. Introduction

Metallothioneins (MT) constitute a well-defined group of low-molecular-weight cysteine-rich metal-binding proteins, widely distributed in nature and generally considered responsible for metal homeostasis and detoxification [1,2] To date most spectroscopic and chemical studies on the metal-binding properties of MT have been carried out with proteins isolated from mammalian organs Relatively few studies have been undertaken with synthetic MT, and even fewer with the protein obtained by genetic engineering With the aim of laying the groundwork for primary structural modifications of MT [3], we used the recombinant DNA approach to synthesize mouse Zn_7-MT and the corresponding α (Zn_4-αMT) and β (Zn_3-βMT) domains Synthesis in *E coli* rendered preparations of high purity and allowed us to report the bioproduction of the β domain for the first time [4] In addition, cadmium titrations of recombinant mouse Zn_7-MT and Zn_4-αMT, followed by absorption and CD spectroscopy, showed that they reproduce the behaviour observed for the native proteins [4,5] Titration of Zn_3-βMT with $CdCl_2$ afforded Cd_3-βMT, Cd_4-βMT and Cd_9-βMT species, which we reported for the first time [4,6]

The synthesis of well-defined, separate α and β domains, particularly the latter, seems to be very promising Recent studies suggest that the two domains of mammalian MT have evolved to perform different functional roles and that they have distinctive kinetic features It has been proposed that the kinetically labile β domain may function in metal exchange processes, whereas the kinetically more stable α domain may be important in detoxification [7] Detailed knowledge of the behaviour of the isolated domains should contribute significantly to our understanding of the entire MT and corroborate the proposed independent behaviour of the α and β domains [8] In addition, it has recently been reported that the structure of the β domain in mammalian MT bears close resemblance to the 3D structure in solution of the same domain in crab MT 1 [7] Accordingly, our understanding of the main functions of crustacean MT is likely to be enhanced by the study of the mammalian β fragment behav-

* Corresponding author Fax +34 93 581 3101, E mail iqipilar@cc uab es

0162 0134/99/$ see front matter
PII S0162 0134(98)10091 0

resin with 2 M HNO_3 were analysed Total sulfur, zinc and copper contents were measured by inductively coupled plasma atomic emission spectrometry (ICP-AES) [16] using a Thermo Jarrell Ash, Polyscan 61E at 182 040 nm (S), 213 856 nm (Zn) and 324 754 nm (Cu) For Ag(I)-containing samples, analogous elemental analyses were performed by inductively coupled plasma mass spectrometry (ICP-MS) on a Perkin-Elmer, Elan-6000 at 33 9679 uma (S) and 106 905 and 108 905 uma (Ag)

2 5 *Molecular mass determination*

The molecular mass of the Cu-βMT species contained in aliquots withdrawn from the titration experiments was determined by electrospray ionization mass spectrometry (ESI-MS) on a Fisons Platform II Instrument (VG Biotech) equipped with the Mass Lynx software provided by the manufacturer, calibrated using horse heart myoglobin (0 1 mg/ml) Two sets of conditions were required depending on the sample For the Cu-βMT samples at pH 7 10 μl of the βMT solution was injected at 25 μl/min, source temperature, 180°C, capillary counter electrode voltage, 4500 V, lens counter electrode voltage, 1000 V, cone potential, 30 V, *m/z* range, 1000 to 1800, scanning rate, 4 s/scan, interscan delay, 0 2 s The liquid carrier was a 5 95 mixture of methanol and 3 mM ammonium formiate/ammonia at pH 7 For samples at pH 3 10 μl of the βMT solution was injected at 30 μl/min, source temperature, 100°C, capillary counter electrode voltage, 4000 V, lens counter electrode voltage, 500 V, cone potential, 70 V, *m/z* range, 1000 to 1800, scanning rate, 3 s/scan, interscan delay, 0 4 s The liquid carrier was a 50 50 mixture of acetonitrile and formic acid at pH 3 The ease of oxidation of Cu^+ in acidic media was avoided by adding mercaptoethanol (0 01%)

Unfortunately, the high concentrations of buffer required by the silver solutions to maintain the pH hampered the characterization of Ag-βMT species by ESI-MS Studies to overcome this problem are now being performed

Throughout this paper we refer to the mol equivalents of metal added in terms of '*x* M^+' to stand for '*x* mol equivalents of M^+' or 'a molar ratio M^+ protein of *x*'

3. Results and discussion

The present study aims to determine the binding abilities of the recombinant βMT fragment in the presence of differing concentrations of Cu^+ and Ag^+ The M^I-βMT species, $M^I = Ag(I)$, Cu(I), have been identified from saturation of the chiral intensity, changes in the UV–Vis absorption spectra and mass determination as increasing amounts of metal ions are added to the protein The analysis of the behaviour of recombinant Zn_7 βMT at pH 7 towards M^I requires knowledge of the role played by the Zn atom In other words, the interpretation of the spectral changes accompanying the addition of M^I to Zn_7 βMT must take into account the spectral signals due to the SCys $\rightarrow Zn^{2+}$ LMCT bands, which can overlap with the new bands related to copper- or silver-thiolate interactions By using apo-βMT, we ensure that the binding site structure depends only on the incoming metal Thus, titrations at two different pH values were carried out These have allowed not only the evaluation of the masking effect of the Zn–SCys coordination but also determination of the stoichiometry of mixed-metal $Zn_4M^I_3$-βMT species

3 1 *Apo-βMT fragment*

Parts (a)–(c) of Fig 1 show the CD, electronic absorption spectra and the difference spectra of the latter recorded during the titration of the recombinant apo-βMT fragment with Cu(I), while parts (a)–(c) of Fig 2 show those recorded during the titration with Ag(I) As expected, the apo-βMT fragment does not have a pronounced CD spectrum (Figs 1(a) and 2(a), line 0) with no signal above 250 nm

3 1 1 *Reaction of recombinant mouse apo βMT with* Cu^+

Upon the addition of Cu(I) to apo-βMT, a derivative-like envelope, 303(+) nm and 326(−) nm, and a very intense band at 263(+) nm develop isodichroically (311 nm) (see Fig 1(a)) and the absorption at 255 nm increases linearly (Fig 1(b)) The CD bands reach their maxima at 6 Cu and the linearity in absorbance is kept until the same number of equivalents of copper are added Also, the difference spectra (Fig 1(c)) show that every Cu(I) added between 1 and 6 contributes equally to the formation of a species with a Cu_6S_9 unit that probably contains a unique type of coordination geometry about Cu Moreover, the molecular weight obtained by ESI-MS of 3532 93 is consistent with the expected molecular weight for a Cu_6-βMT species of 3533 82 (apo-βMT + 6Cu − 6H)

The addition of increments of Cu(I) to Cu_6-βMT up to one Cu(I) reveals an extensive rearrangement of the Cu_6-βMT aggregate with the incorporation of the seventh Cu(I) (Fig 1(a)) Thus, there is a development of new bands at 237(+), 336(+), 368(+) and 400(−) nm and the intense band centred at 263(+) nm decreases in intensity, while it shifts to 259(+) nm The absorption spectra and the difference absorption spectra (Fig 1(b) and (c), respectively) show that during this phase there are significant contributions at wavelengths not observed before 235, 285 and 335 nm These are consistent with the changes observed in the CD spectra and indicate formation of new Cu–S coordination environments, which give rise to a new species, of stoichiometry Cu_7-βMT The presence of this species was confirmed by ESI MS yielding a molecular weight of 3595 86, in comparison with the expected value for Cu_7-βMT species of 3596 36 (apo-βMT + 7Cu − 7H)

Over 7 Cu^+ added, the absorption spectra, with an isosbestic point at 320 nm and their difference spectra are indicative of copper binding to Cu_7 βMT until 10 Cu^+ added (see Fig 1(b) and (c)) These show the contribution of the Cu–S bonds in the high energy region and also a loss of

iour. However, until recently, the study of the β domain was hindered by the difficulties associated with its synthesis by means of the solid-phase or solution fragment-condensation techniques, or with its recovery and purification from living organisms.

Despite the high level of similarity found between the behaviour of native versus recombinant MT towards Cd(II) [4,5], the results obtained with Hg(II) [9] were different from those reported for the native proteins [10]. This finding prompted us to extend our studies to monovalent metal ions such as Cu(I) and Ag(I). Copper metallothioneins have been most extensively studied, mainly in vitro, yielding a variety of results on the Cu-binding stoichiometry [11–13]. Moreover, the spectral data for silver binding are claimed to be of interest, as they are believed to provide information on copper binding to MT. According to the literature, the close similarities displayed by Cu(I) and Ag(I) in their interaction with MT support the use of Ag^+ as an NMR-active analogue of Cu^+ in structural studies [13]. In this paper, we examine and compare the Cu(I) and Ag(I) binding abilities of the recombinant mouse β fragment at different pH values through the pattern of the CD and UV–Vis absorption spectra recorded during the corresponding titrations. Although little information is available on M^I-βMT (M^I=Cu, Ag) species, there appear to be differences in the behaviour of recombinant protein and native protein in their presence.

2. Experimental

2.1. Protein preparation and characterization

Expression assays, fermentator-scale cultures, purification of the fusion protein and recovery and analysis of the recombinant mouse Zn_3-βMT 1 fragment were performed as previously described [4]. Accordingly, the Zn_3-βMT species was obtained in a Tris–HCl buffer (50 mM, pH=7) except for those samples to be used in the Ag(I) titrations, which were obtained in Tris–$HClO_4$ (50 mM, pH=7), to avoid precipitation of AgCl. All protein solutions had a final concentration of about 300 μM. These were diluted and titrated with freshly prepared solutions of $[Cu(CH_3CN)_4]^+$ in CH_3CN/H_2O or Ag^+ in Milli-Q purified water at 25°C.

The apo-βMT proteins were prepared by acidification of the recombinant material with 10^{-2} M HCl until the pH was 3 for the Cu(I) titrations and with $ClCH_2COOH$/$ClCH_2COONa$ buffer at pH 2.5 for the Ag(I) titrations. At pH lower than 3.5 the Zn_3-βMT is entirely demetalled, according to the CD spectrum. In contrast, Cu(I) and Ag(I) can bind to S-Cys at low pH down to 1.5.

2.2. Metal solutions

Glassware, solutions and Chelex-100 used in metal-ion-binding studies were prepared as described [4]. Due to the known sensitivity of Cu(I) to both oxidation and disproportionation, the solutions of Cu^+ were prepared from $[Cu(CH_3CN)_4]ClO_4$ [14], in 30% (v/v) CH_3CN/H_2O. The concentration of copper was quantified by AAS using a Perkin-Elmer 2100 atomic absorption spectrometer. The absence of detectable Cu^{2+} in the freshly prepared Cu(I) solution, and after use as a titrating agent, was confirmed by the lack of EPR signal (Bruker ESP 300E; at 77 K). To avoid hydrolysis, Ag^+ solutions were prepared by dissolving $AgClO_4$ in aqueous $HClO_4$ of pH 0.5 and standardized by potentiometric titrations against standard NaCl solution [15]. The concentration of the Cu^+ or Ag^+ solution used as titrating agent was in the range 10^{-2}–10^{-3} M.

2.3. Metal-ion-binding reactions

Metal-binding experiments were carried out by sequentially adding molar ratio aliquots of concentrated Cu^+ or Ag^+ solution to a single solution of either Zn_3-βMT or apo-βMT. For each addition, the protein sample was allowed to react with the metal ion until the CD features became stable. Thus, the CD spectra were recorded every 10 min until subsequent CD spectra were fully coincident. Absorption studies were conducted in parallel with CD studies. At some points during the titrations, a 10 μl aliquot was withdrawn and saved for mass determination.

All manipulations involving the metal and protein solutions were performed in argon atmosphere and titrations were carried out at least in duplicate to ensure the reproducibility of each single point.

The pH for all experiments remained constant throughout. This was achieved differently in the case of Cu(I) or Ag(I) titrations. In Cu^+ titrations no buffers were needed to maintain the initial pH of the protein solution, 7 or 3. In contrast, the acidity of the Ag(I) solution required the addition of appropriate buffer solutions of Tris–$HClO_4$ (250 mM, pH 7.5) or $ClCH_2COOH$/NaOH (20 mM, pH 2.5).

The electronic absorption measurements were performed in 1 cm capped quartz cuvettes on an HP-8452A diode array UV–Vis spectrophotometer. A Jasco spectropolarimeter (model J-715) interfaced to a computer was used for CD measurements. A Peltier PTC-351 S was used to maintain the temperature constant at 25°C in all the experiments. Both types of spectrum were corrected for the dilution effects and processed using the program GRAMS 32.

2.4. Chelex-100 experiments

The possibility that Zn(II) was bound to the protein in the M^I-βMT species (M^I=Cu or Ag) formed in the titrations of Zn_3-βMT at pH=7 was considered. In order to determine the zinc content in the $Zn_xM_y^I$-βMT species, a second titration was carried out until the suspected mixed-metal species was formed. Then, a small quantity of Chelex-100 was added to the solution following a procedure described elsewhere [4] and the sulfur, zinc and copper or silver contents of the supernatant and of the solutions obtained after treatment of the

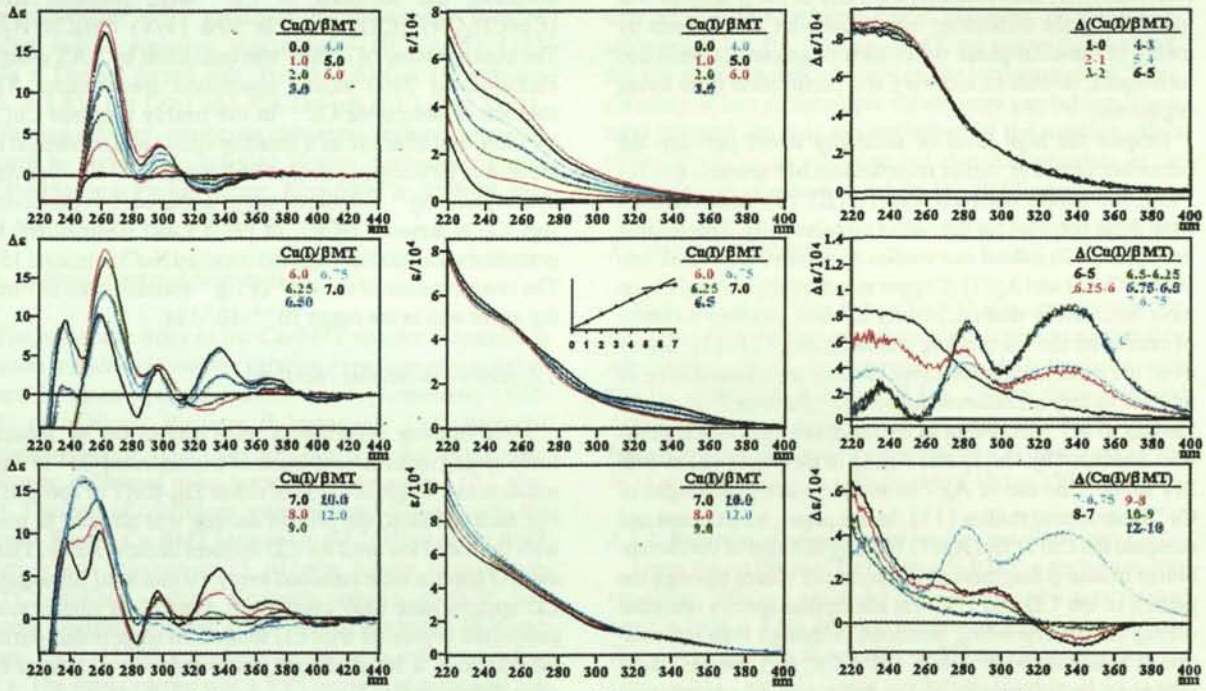

Fig. 1. Cu(I) titration of a 1.98×10^{-5} M solution of recombinant apo-βMT at pH 3: (a) CD spectra; (b) UV–Vis absorption spectra; (c) difference absorption spectra obtained by subtracting the successive spectra of (b). For comparison, their intensities have been normalized with respect to one molar addition. The Cu^+ to MT molar ratios are indicated within each frame. The inset in (b) shows the variation of the absorbance at 255 nm between 0 and 7 equivalents of Cu^+ added.

absorbance centred at 340 nm, which could indicate the loss of a particular type of copper coordination constituted in the anterior phase. The CD spectra during this phase show that the bands at 297(+), 336(+), 368(+) and 400(−) collapse, while the two bands at 237(+) and 259(+) nm give rise to a unique band centred at 245(+) nm (Fig. 1(a)).

3.1.2. Reaction of recombinant mouse apo-βMT with Ag^+

The spectral data shown for the apo-βMT fragment titration with Ag^+ (Fig. 2) are unusually weak although the protein concentration was doubled to enhance the signal-to-noise ratio. The low intensities of these spectra contrast with the data we obtained when Ag^+ binds to Zn_3-βMT, but are consistent with those reported for the titration of the apo form of native fragments with silver [17]. Moreover, CD and UV–Vis data obtained in this work do not resemble those recorded for Cu^+ either in the shape of the spectral envelopes or in their intensities. The CD data (Fig. 2(a)) show formation of Ag_3-βMT with bands at 250(+) and 290(+) nm. Ag_3-βMT is replaced by a new species, Ag_6-βMT, which is characterized by a CD spectrum with maxima at 246(+), 270(+) and 295(+) nm. Finally, we can associate the broad bands at 276(+) and 350(−) with formation of Ag_9-βMT.

UV–Vis absorption spectra show a broad envelope that starts at about 380 nm and extends into the far-UV (Fig. 2(b)). The intensity of the absorption in the 250–290 nm region increases linearly with increasing Ag(I) equivalents up to 6 Ag^+. The slope of the absorbance intensity clearly changes with the addition of the seventh equivalent. This finding is corroborated by the difference spectra (Fig. 2(c)) which indicate a cooperative effect for the first 3 Ag(I) equivalents added, similar behaviour from 3 to 6 Ag^+, and a smaller increment in absorbance due to the last equivalents. Saturation is reached for 9 Ag^+. Unfortunately, the difference spectra are not well resolved and they only reveal a generalized absorption between 230 and 400 nm, with a maximum centred at 230 nm, which could indicate the same type of Ag–S coordination environment in all the species formed.

3.2. Zn_3-βMT fragment

Parts (a)–(c) of Fig. 3 show the CD, electronic absorption spectra and the difference spectra of the latter recorded during the titration of the recombinant Zn_3-βMT fragment with Cu(I), while parts (a)–(c) of Fig. 4 show those recorded during the titration with Ag(I). As expected, the Zn_3-βMT species shows the characteristic CD feature (Figs. 3(a) and 4(a), line 0), already described elsewhere [4].

3.2.1. Reaction of recombinant mouse Zn_3-βMT with Cu^+

Intense dichroic bands develop in the CD spectrum during the addition of the first 4 Cu(I) equivalents to Zn_3-βMT. Fig. 3(a) shows that the 247(+) nm CD band characteristic of Zn_3-βMT increases its intensity and red-shifts up to 258(+)

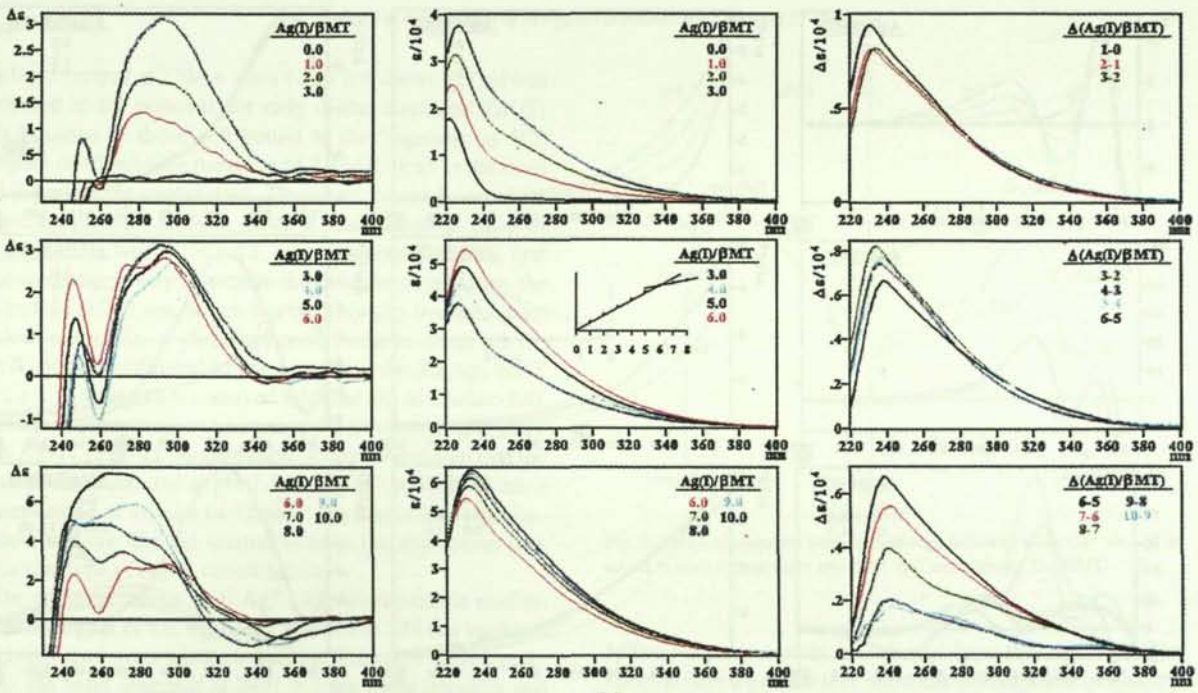

Fig. 2. Ag(I) titration of a 4.00×10^{-5} M solution of recombinant apo-βMT at pH 2.5: (a) CD spectra; (b) UV–Vis absorption spectra; (c) difference absorption spectra obtained by subtracting the successive spectra of (b). The Ag^+ to MT molar ratios are indicated within each frame. The inset in (b) shows the variation of the absorbance at 250 nm between 0 and 8 equivalents of Ag^+ added.

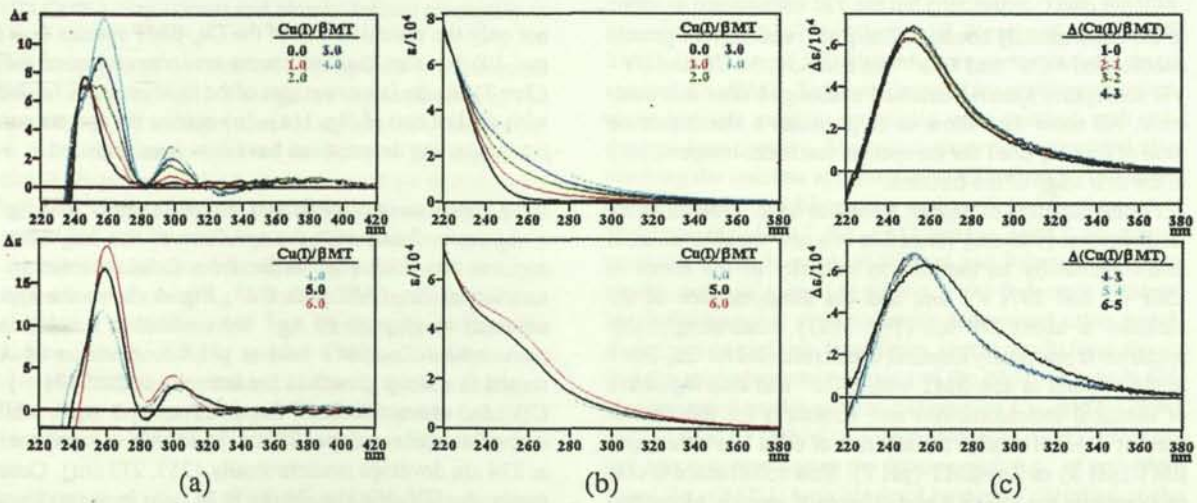

Fig. 3. Cu(I) titration of a 1.95×10^{-5} M solution of recombinant Zn_3-βMT at pH 7: (a) CD spectra; (b) UV–Vis absorption spectra; (c) difference absorption spectra obtained by subtracting the successive spectra of (b). The Cu^+ to MT molar ratios are indicated within each frame. The spectra corresponding to the last phases of the titration have been omitted as they coincide with the last two of Fig. 1(a)–(c).

maintaining a shoulder at about 240 nm, while two bands at 297(+) and 327(−) nm gradually intensify through isodichroic points at 248, 282 and 315 nm. The absorption UV–Vis spectra (Fig. 3(b)) and their difference spectra (Fig. 3(c)) indicate an isosbestic (224 nm) increase in absorbance at about 250 nm and also a cooperative effect in the binding of these 4 Cu(I). The negative increase in absorbance below 230 nm can be attributed to the superposition of the loss of Zn–S chromophores (240 nm) over the gain due to the newly formed Cu–S chromophores. In a parallel titration, Chelex-100 was added after incorporation of the first four Cu^+ in order to bind the displaced Zn^{2+} ions (data not shown), according to the method described previously [4]. Analytical results indicated that the chelating resin sequestered 2 Zn^{2+}

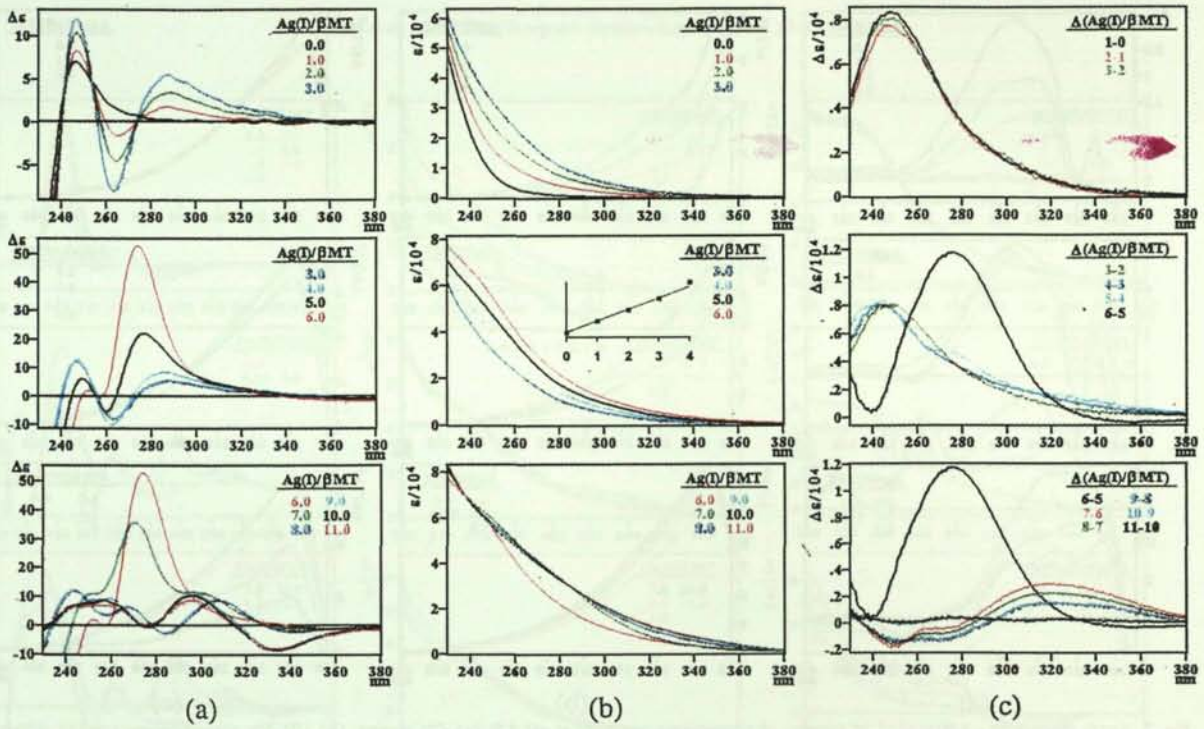

Fig. 4. Ag(I) titration of a 1.99×10^{-5} M solution of recombinant Zn_3-βMT at pH 7.5: (a) CD spectra; (b) UV–Vis absorption spectra; (c) difference absorption spectra obtained by subtracting the successive spectra of (b). The Ag^+ to MT molar ratios are indicated within each frame. The inset in (b) shows the variation of the absorbance at 263 nm between 0 and 4 equivalents of Ag^+ added.

of the three initially bound in Zn_3-βMT, and that the protein coordinated 4 Cu^+ and 1 Zn^{2+}. In addition, the CD and UV–Vis absorption spectra remained unchanged after this treatment. All these data allow us to postulate a stoichiometric ratio of Zn_1Cu_4-βMT for the species that forms cooperatively in the first stage of the titration.

Further addition of copper, from 4 to 6 Cu^+, results in the isodichroical (346 nm) formation of a new species, which is characterized by an increase in intensity of the bands at 258(+) and 297(+) nm, and the disappearance of the shoulder at about 240 nm (Fig. 3(a)). Interestingly, this spectrum is practically identical to that recorded for Cu_6-βMT in the titration of apo-βMT with 6 Cu^+ and thus indicative of identical stoichiometries and structures for the species present in solution after the addition of 6 Cu^+ to either apo-βMT (pH 3) or Zn_3-βMT (pH 7). This coincidence is corroborated by the UV–Vis and difference spectra. Moreover, subsequent additions of Cu(I) to Cu_6-βMT give rise to nearly identical spectral patterns (CD, UV–Vis absorption and difference spectra) regardless of the pH (7 or 3) of the titration. Molecular weight measurements for Cu_6-βMT and Cu_7-βMT species are in good agreement with the values found in the titration of the apo-βMT fragment (see above). Accordingly, titrations carried out at pH 3 and pH 7 reveal that the series of species Cu_6-βMT, Cu_7-βMT, Cu_{10}-βMT form in sequence as Cu^+ is added to either apo-βMT or Zn_3-βMT, respectively. The similarity of the CD spectral traces indicates that not only the stoichiometry of the Cu_x-βMT species ($x=6$, 7 and 10) but also their structures are independent of the pH (3 or 7). As the last two stages of the titration at pH 7 coincide with the last two of Fig. 1(a)–(c) neither the spectra nor the corresponding descriptions have now been included.

3.2.2. *Reaction of recombinant mouse Zn_3-βMT with Ag^+*

Again, as found with the apo form of this fragment, the spectral data with Ag^+ differ from those recorded in the titration of Zn_3-βMT with Cu^+. Fig. 4 shows the spectra obtained as aliquots of Ag^+ were added to a solution of recombinant Zn_3-βMT held at pH 7.5. Addition of Ag^+ results in a steep growth in the intensity of the 247(+) nm CD band characteristic of Zn_3-βMT up to 3 Ag^+, while a derivative-like envelope (263(−) and 288(+) nm) centred at 274 nm develops isodichroically (253, 273 nm). Concurrently, the UV–Vis absorbance at 263 nm increases linearly up to 3 Ag^+ (Fig. 4(b)) and the corresponding difference spectra (Fig. 4(c)) are coincident. All these data show a high cooperativity at this stage of the titration.

To analyse the influence of Zn^{2+} ions on the Ag-βMT species formed, Chelex was added to the Zn_3-βMT solution after the addition of 3 Ag^+ in a parallel titration. Surprisingly, unlike the behaviour observed in the Cu^+ titration, the UV–Vis absorption and CD spectra changed considerably after addition of the resin: the 247(+) CD band decreased in intensity while the exciton coupling disappeared to give rise

to a band centred at 279(+) nm (data not shown). This was attributed to the removal not only of the displaced Zn(II) ions but also of those still bound to the fragment, as ICP analyses confirmed the presence of 3 Zn(II) ions in the resin and 3 Ag^+ in the supernatant. Therefore, on the basis of the spectroscopic and analytic data, a stoichiometric ratio of Zn_xAg_3-βMT, where $1 \leq x \leq 3$, can be proposed for the first species cooperatively formed in the titration. In addition, the absorption at 247 nm, which has traditionally been assigned exclusively to Zn–S chromophores, remains when all the Zn(II) ions coordinated to the protein in the Zn_xAg_3-βMT ($1 \leq x \leq 3$) species are removed with the aid of Chelex-100. The same absorption can be seen in the titration of apo-βMT with Ag(I) (Fig. 2). Accordingly, it can be deduced that the spectral data recorded at pH 7.5 in the 247 nm region are a superposition of at least two bands: the first is from the Zn–S chromophore and the second reflects the absorption of a particular type of Ag–S coordination.

On addition from 3 to 6 Ag^+, the characteristic exciton coupling signal of Zn_xAg_3-βMT centred at 274 nm vanishes to give rise to a very intense band at the same wavelength. Also, the band observed at 247(+) nm loses intensity and disappears, indicating the loss of the coordinated Zn(II) ions. The new Gaussian-shaped band can be taken as the fingerprint of the Ag_6-βMT species. Although the UV–Vis spectra are not conclusive in this phase of the titration, their difference spectra show a very intense and clearly defined absorption at 276 nm.

The last phase of the titration corresponds to subsequent additions up to 11 Ag^+. The spectra are indicative of the complexity of the changes that take place in solution and show that saturation is achieved for 9 Ag^+. The Ag_9-βMT species is characterized by a spectral envelope that shows a broad band centred at 259(+) nm and a derivative envelope centred at 317 nm. The difference spectra indicate the loss of the Ag–S chromophores formed in the previous phases and the appearance of a third Ag–S environment characterized by an absorption centred at 319 nm. Comparison of the CD envelopes corresponding to species with the same stoichiometric ratio with those obtained in the titration of the apo-βMT strongly suggests that each Ag-βMT species adopts a distinct structure at each pH value (compare Figs. 2(a) and 4(a)).

In summary, on the basis of the spectroscopic data and their comparison at neutral and acidic pH, we propose the reaction pathways given in Fig. 5. These show that the recombinant βMT fragment binds Ag^+ and Cu^+ in several stages, with distinct species forming at Ag_6 and Ag_9, whose structure depends on the pH (2.5 or 7.5), and Cu_6, Cu_7 and Cu_{10} as pH-independent structures (in the range 3 to 7). Also, two mixed-metal species have been characterized, Zn_1Cu_4 and Zn_xAg_3 ($1 \leq x \leq 3$), which introduces interesting questions about the charge compensation-based displacement of Zn^{2+} from MT by monovalent metal ions [18] and about the ability of silver to afford mixed-metal MT species [13]. These results clearly indicate that the behaviour of copper towards

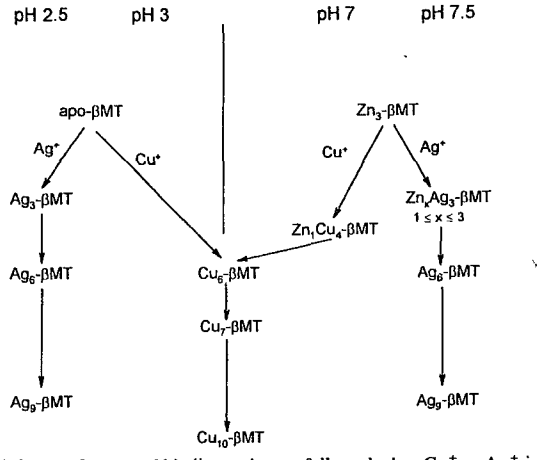

Fig. 5. Series of proposed binding pathways followed when Cu^+ or Ag^+ is added to both recombinant apo-βMT and recombinant Zn_3-βMT.

MT cannot necessarily be inferred from that of silver. The spectral data we report here show the development of maxima at molar ratios (3, 6 and 9) that appear to be reasonable for Ag-βMT complexes, differing from those values determined for Cu^+ binding to the β fragment (6, 7 and 10).

Up to now literature data on the copper-binding stoichiometry in mammalian MT are not conclusive. Thus, the titration of the chemically synthesized β domain of rat liver MT 2 with Cu(I) at pH 2.5 allowed characterization of a single species, Cu_6-βMT. This was detected by emission spectroscopy; but CD maxima intensities were reached with only three to four coppers. The two to three coppers added after reaching the maxima appeared to be CD-silent [12]. On the other hand, the stoichiometries we have found for the species with more than 6 Cu^+, Cu_7-βMT and Cu_{10}-βMT, are consistent with the early work of Nielson and Winge [8], where similar ratios of copper to protein in the β domain obtained by partial enzymic digestion were determined using metal-dependent proteolysis. In addition, recent results have shown that the recombinant expression of the βMT domain in Cu-supplemented media affords mixtures of Cu_6-βMT (25%) and Cu_7-βMT (75%) [19]. With respect to Ag(I), CD spectral data recorded during the titration with Ag^+ of apo-βMT 1 and Zn_3-βMT 1, both obtained by partial digestion of the native protein, allowed characterization of the Ag_3-βMT and Ag_6-βMT, and Ag_6-βMT species, respectively [17,18]. However, the number of species, their stoichiometry and corresponding spectral envelopes do not coincide with those found with the recombinant protein. We have observed that the pH plays a significant role in the metallothionein metal-binding pathways. Moreover, reactions of recombinant MT fragments with Cu^+ and Ag^+, like the reaction of recombinant MT with Hg^{2+} [9], are not as instantaneous as those reported for Cd^{2+} [4,5]. Thus, provision of the required stabilization time for the formation of complex species and constancy of pH during the titration are fundamental to

achieve a precise indication of the stoichiometric ratios of the Ag- and Cu-MT species.

Due to the differences observed in the abilities of Cu(I) and Ag(I) to bind to recombinant βMT, the αMT and the entire MT have also been studied. Again, the results differ from those reported in the literature for the native proteins and show that the recombinant proteins bind copper and silver differently. A detailed report on these findings is in preparation.

The CD, UV and, above all, difference absorption spectra have allowed us to identify precise UV–Vis absorptions during the titrations of the recombinant βMT fragment with monovalent metal ions In the case of silver, absorptions at three distinct wavelengths have been recorded: 248 (formation of Zn_xAg_3-βMT), 276 (formation of Ag_6-βMT) and 319 nm (formation of Ag_9-βMT), the positions of which clearly parallel the features observed in the CD spectrum (Fig. 4). Interestingly, the appearance of each of these absorptions implies the disappearance of the previous one. Thus, it is tempting to speculate that each energy corresponds to a different geometry of coordination about silver, which in turn may be related to the metal-to-SCys molar ratio. As a general pattern, with increasing M(I)/βMT stoichiometry the stereochemistry around the metal might change from tetrahedral to diagonal through trigonal-planar coordination. Conversely, the addition of copper to recombinant βMT gives rise to a more complex pattern of difference spectra: a broad absorption centred at 235 (formation of Cu_6-βMT), three simultaneous absorptions at 235, 285 and 335 (formation of Cu_7-βMT) and weak absorptions at 265 and 295 nm (formation of Cu_{10}-βMT) (Fig. 1) Traditionally, in the Cu(I)-containing mammalian metallothioneins it has been proposed that the Cu(I) is trigonally coordinated by the SCys ligands [20,21]. However, the structural diversity of copper and silver thiolates [22], the lack of established correlations between their structure and physical properties [23] and the few conclusive assignments of the different absorption energies associated with the manifold coordination numbers of these metal ions in protein environments [11] do not give us enough evidence to support a specific type of coordination for the M^I-βMT species reported in this study.

4. Abbreviations

EPR	electron paramagnetic resonance
ESI-MS	electrospray ionization mass spectrometry
ICP-AES	inductively coupled plasma atomic emission spectrometry
ICP-MS	inductively coupled plasma mass spectrometry

Acknowledgements

This work was supported through Projects PB97-0216 and PN96-0225. M.C. is indebted to the Fundación Caja de Madrid for a post-doctoral fellowship and R.B. to the Comissionat per a Universitats i Recerca de la Generalitat de Catalunya (CIRIT) for a pre-doctoral scholarship. We acknowledge the Serveis Científico-Tècnics, UB (ESI-MS, ICP-AES, ICP-MS), the Servei d'Anàlisi Química, UAB (AAS, CD) and the ICMAB (EPR) for allocating instrument time.

References

[1] J H R Kagi, A Schaffer, Biochemistry 27 (1988) 8509
[2] D M Templeton, M G Cherian, Methods Enzymol 205 (1991) 11
[3] N Romero-Isart, N Cols, M K Termansen, J L Gelpí, R González-Duarte, S Atrian, M Capdevila, P González Duarte, Eur J Biochem 259 (1999) 519
[4] M Capdevila, N Romero-Isart, R González-Duarte, S Atrian, P González-Duarte, Cell Mol Life Sci 53 (1997) 681
[5] N Cols, N Romero-Isart, M Capdevila, B Oliva, P González-Duarte, R González-Duarte, S Atrian, J Inorg Biochem 68 (1997) 157
[6] M Capdevila, N Romero-Isart, N Cols, S Atrian, M J Stillman, R González-Duarte, P González-Duarte, An Quim Int Ed 92 (1996) 199
[7] S S Narula, M Brouwer, Y Hua, I M Armitage, Biochemistry 34 (1995) 620
[8] K B Nielson, D R Winge, J Biol Chem 260 (1985) 8698
[9] S Atrian, R Bofill, M Capdevila, N Cols, P González Duarte, R González-Duarte, A Leiva, O Palacios, N Romero-Isart, in C Klaassen (Ed), Metallothionein IV, Birkhauser, Basel, 1998, p 55
[10] W Lu, M J Stillman, J Am Chem Soc 115 (1993) 3291
[11] D L Pountney, I Schauwecker, J Zarn, M Vašák, Biochemistry 33 (1994) 9699
[12] Y J Li, U Weser, Inorg Chem 31 (1992) 5526
[13] H Li, J D Otvos, Biochemistry 35 (1996) 13929
[14] G J Kubas, Inorg Synth 19 (1979) 90
[15] I M Kolthoff, E B Sandell, E J Meehan, S Bruckenstein, Quantitative Chemical Analysis, Macmillan, New York, 1969
[16] J Bongers, C D Walton, D E Richardson, J U Bell, Anal Chem 60 (1988) 2683
[17] A J Zelazowsky, Z Gasyna, M J Stillman, J Biol Chem 264 (1989) 17091
[18] A Zelazowski, M J Stillman, Inorg Chem 31 (1992) 3363
[19] N Cols, N Romero-Isart, R Bofill, M Capdevila, P González-Duarte, R González Duarte, S Atrian, Protein Eng (1999) in press
[20] G N George, D Winge, C D Stout, S P Cramer, J Inorg Biochem 27 (1986) 213
[21] A Presta, A R Green, A Zelazowski, M J Stillman, Eur J Biochem 227 (1995) 226
[22] I G Dance, K Fisher, G Lee, in M J Stillman, F C Shaw III, K T Suzuki (Eds), Metallothioneins, VCH, New York, 1992, pp 284–323
[23] H G Fijolek, P González Duarte, S H Park, S L Suib, M J Natan, Inorg Chem 36 (1997) 5299

Article 2

N. Cols, N. Romero-Isart, R. Bofill, M. Capdevila, P. Gonzàlez-Duarte, R. Gonzàlez-Duarte, S. Atrian.

In vivo copper- and cadmium-binding ability of mammalian metallothionein β domain.

Prot. Engng., **1999**, *12*, 265-269.

Protein Engineering vol 12 no 3 pp 265–269, 1999

In vivo copper- and cadmium-binding ability of mammalian metallothionein β domain

Neus Cols*, Núria Romero-Isart[1,*], Roger Bofill[1], Mercè Capdevila[1], Pilar Gonzàlez-Duarte[1], Roser Gonzàlez-Duarte and Sílvia Atrian[2]

Departament de Genetica, Facultat de Biologia Universitat de Barcelona Av Diagonal 645, 08071 Barcelona, Spain and [1]Departament de Quimica, Universitat Autonoma de Barcelona, 08193 Bellaterra, Barcelona, Spain

[2]To whom correspondence should be addressed

*Made equal contributions to this study

The β domain of mouse metallothionein 1 (βMT) was synthesized in *Escherichia coli* cells grown in the presence of copper or cadmium. Homogenous preparations of Cu–βMT and Cd–βMT were used to characterize the corresponding *in vivo*-conformed metal-clusters, and to compare them with the species obtained *in vitro* by metal replacement to a canonical Zn_3–βMT structure. The copper-containing βMT clusters formed inside the cells were very stable. In contrast, the nascent β peptide, although it showed cadmium binding ability, produced a highly unstable species, whose stoichiometry depended upon culture conditions. The absence of βMT protein in *E.coli* protease-proficient hosts grown in cadmium-supplemented medium pointed to drastic proteolysis of a poorly folded β peptide, somehow enhanced by the presence of cadmium. Possible functional and evolutionary implications of the bioactivity of mammalian βMT in the presence of monovalent and divalent metal ions are discussed.

Keywords β domain/*in vivo* copper binding/*in vivo* cadmium binding/metallothionein/recombinant expression

Introduction

Non-enzymatic metalloproteins are both storage/transport agents for essential metals inside organisms and defence mechanisms against xenobiotic elements Among them, metallothioneins (MT) show the highest and most general metal coordinating capacity They are small (60–65 residues), cysteine-rich (up to 30% in mammals) proteins notably abundant in animals, although also reported in other phyla The observation that in response to metal exposure, the physiological levels of MT increase dramatically has led to the assignment of a protective and detoxifying function for MT Besides, a house-keeping role on metal homeostasis has also recently been claimed (Kagi, 1993)

Mammalian MT, the most evolved form, folds over metal atoms constituting two domains β, the N-terminal half, and α, the C-terminal half The β domain includes nine Cys residues, mostly in an alternate pattern, -NCNCN- or -NCNNCN-, and binds three divalent ions (Zn or Cd), giving rise to a $M_3(SCys)_9$ aggregate where each metal ion is tetrahedrally coordinated The α domain comprises 11 Cys, in an -NCNCN- or -NCCNCC- array, and it is able to bind four divalent ions tetrahedrally, affording a $M_4(SCys)_{11}$ aggregate (Otvos and Armitage, 1980, Furey *et al*, 1986) These features are generally used to classify non-mammalian MT as α *domain-like* or β *domain like* peptides (Nemer *et al*, 1985) According to this criterion, yeast and fungal MT, the most primitive eukaryotic forms, are constituted by single β domains (Peterson *et al*, 1996), crustacean MT has two (β–β) domains (Narula *et al*, 1995), echinodermal MT is made of two (α–β) domains (Wang *et al*, 1995) and vertebrate MT shows two (β–α) domains From these data, it seems plausible that duplication and divergence of an ancestral β unit may have led to the present situation in crustacean, echinodermal and vertebrates. If we consider their metal-chelating properties, fungal MT appears optimized for Cu-binding (Winge *et al*, 1985), whereas divalent ions, especially cadmium, are preferentially bound by the mammalian forms Not only has the high stability of the Cd_4–αMT mammalian cluster been assessed *in vitro* (Bernhard *et al*, 1986, Capdevila *et al*, 1997), but dramatic decreases in cadmium resistance in transformed cells has also been reported for mutants where the α domain is nonfunctional (Chernaik and Huang, 1991) A housekeeping metal-regulatory role for MT in lower organisms is supported by the affinity of native βMT forms for physiological metals (Cu, Zn) This function may have been extended to a detoxifying capacity, mainly acquired by the new α domain Coordination studies have shown the differential chelating behaviour of both MT portions towards these metals *in vitro* (Nielson and Winge, 1984, Nielson *et al*, 1985, Okada *et al*, 1985, 1986, Li and Otvos, 1996), but genetic engineering strategies allow characterization of the metal binding ability *in vivo* We have previously shown that both mammalian recombinant domains and the entire MT are able to coordinate Zn, leading to Zn_3–βMT, Zn_4–αMT and Zn_7–MT respectively (Capdevila *et al*, 1997, Cols *et al*, 1997), and time-coincident studies have also been reported for the same species (Xiong and Ru, 1997) The corresponding MT aggregates were recovered from a GST–MT fusion construct rendered by a bacterial heterologous expression system, previously described for plant and cyanobacterial MT (Tommey *et al*, 1991, Shi *et al*, 1992) Although the recombinant Cd_4–αMT complex has been described, attempts to synthesize heterologous βMT in Cd-supplemented media were reported unsuccessful (Sewell *et al*, 1995, Kurasaki *et al*, 1996, Kurasaki *et al*, 1997) Furthermore, no data about *in vivo* mammalian α or βMT copper binding have been reported up to now Here we describe the synthesis of mouse βMT in *E coli* cells grown in the presence of Cu and Cd, and provide data on the corresponding metal clusters The factors inhibiting expression when cadmium is present in the culture medium have also been addressed

Materials and methods

Recombinant expression and purification of MT β domain as different metal complexes

In order to express the βMT domain as a Cu- and Cd-complex, *E coli* strains JM105 (protease proficient) and BL21 (lon and ompT protease deficient) were transformed with the

plasmid pGEX-4T-βMT (Capdevila *et al.*, 1997). To synthesize Cu–βMT or Cd–βMT, *E.coli* cultures were supplemented with $CuSO_4$ or $CdCl_2$, to final concentrations of 300 and 500 μM Cu^{2+}, or 100 and 300 μM Cd^{2+}, respectively. To verify whether βMT production was possible in non-metal-supplemented media, cultures without added metals were performed. As a control, the αMT domain was also assayed for expression in cadmium-supplemented media. Basic procedures for the expression and purification of the βMT–metal complexes were as reported (Capdevila *et al.*, 1997). Aliquots of the protein-containing FPLC fractions were separated by 15% SDS–PAGE, which were stained with Coomassie blue. Positive samples were pooled, and aliquots were stored at –70°C for further analysis.

Analysis of the binding properties of in vivo synthesized Cu–βMT and Cd–βMT

Inductively coupled plasma-atomic emission spectrometry (ICP-AES), in a Thermo Jarrell Ash, Polyscan 61E (measuring S at 182.0 nm, Zn at 231.8 nm, Cd at 228.8 nm and Cu at 324.7 nm) was used to assess S, Zn, Cd and Cu contents, to calculate the amount of protein present in the preparation and the metal-to-protein ratios. Additionally, the reaction with DTNB [5,5′-dithiobis(nitrobenzoic acid)], as described elsewhere (Birchmeier and Christen, 1971), allowed us to determine the percentage of thiol groups over total sulfur in our samples except for those containing Cu, as it is widely accepted that the presence of this metal in MT prevents determination of SH content by Ellman's method (Winge, 1991).

Electrospray ionization mass spectrometry (ESI-MS) was performed on a Platform II (Micromass) equipped with Max Lynx software, calibrated using horse heart myoglobin (0.1 mg/ml). Different sets of assay conditions were required depending on the sample. For apo-βMT: source temperature, 60°C; capillary-counterelectrode voltage, 3.5 kV; lens-counterelectrode voltage, 0.5 kV; cone potential, 40 V; m/z range, 600 to 1700; scan rate, 4 s/scan; interscan delay, 0.2 s; and the carrier, a 1:1 mixture of acetonitrile and a 0.05% trifluoroacetic acid solution, at pH 2.5. For Cu–βMT: source temperature, 120°C; capillary-counterelectrode voltage, 4.5 kV; lens-counterelectrode voltage, 1 kV; cone potential, 35 V; m/z range, 700 to 2000; scan rate, 4 s/scan; interscan delay, 0.2 s; and the carrier, a 5:95 solution of methanol and 3 mM ammonium formate/ammonia, at pH 7.0. To avoid the masking effect of Tris over Cu–βMT, samples were dialyzed for 90 min against 2.5 mM Tris–HCl, pH 7.0, using Pierce Slide-A-Lyzer membranes (cut-off: 2000) prior to injection. For Cd–βMT: source temperature, 120°C; capillary-counterelectrode voltage, 4.5 kV; lens-counterelectrode voltage, 1 kV; cone potential, 35 V; m/z range, 1000 to 1800; scan rate, 5 s/scan; interscan delay, 0.5 s; and the carrier, a 5:95 solution of methanol and 3 mM ammonium formate/ammonia at pH 7.5.

Electronic absorption measurements were performed on a HP-8452A Diode array UV-visible spectrophotometer. A Jasco Spectropolarimeter (J-715) interfaced to a computer (GRAMS/32 Software) was used for circular dichroism determinations.

Results

Expression of the βMT domain in the presence of different metals

We had previously shown that successful biosynthesis of the βMT domain, as well as that of αMT, was achieved in Zn-supplemented media using both JM105 and BL21 *E.coli* strains, and as expected the latter always rendered higher protein yield (Capdevila *et al.*, 1997). In the present study, however, markedly different results were obtained for the synthesis of βMT in the presence of other metals. When the pGEX-4T-βMT construct was expressed in *E.coli* JM105, the GST–βMT fusion protein was recovered at comparable yields in both non-metal and Zn^{2+}-supplemented media (Figure 1, lanes 2 and 3); showed significant levels of synthesis when the medium was Cu^{2+}-supplemented (lane 5); and was almost negligible in the assays of Cd^{2+}-supplemented media (lane 4). Unlike Zn–MT and Cd–MT, the yield of Cu(I)–MT synthesis is affected by the required reduction of the Cu(II) available to the *E.coli* cell prior to the formation of the corresponding clusters. To further test the behaviour of the recombinant βMT in the presence of cadmium, the same construct was transformed and tested for expression in BL21 cells. Figure 2 shows the PAGE results for GST–βMT, and GST–αMT as a control, for the two *E.coli* strains in Cd-supplemented media. It is well reported that pure, homogenous, metal-loaded MT migrates heterogeneously on SDS–PAGE, often rendering diffuse bands, and shows an electrophoretic mobility much lower (apparent 14 kDa) than that corresponding to the molecular mass of the apo-form (3.5 kDa), due to the fact that the SDS sample and gel conditions are not able to cause full denaturation of the metal–protein clusters, and thus the protein migrates as a metal aggregate along the gel (McCormick *et al.*, 1991). The behaviour of the αMT fusion protein was similar to that in Zn medium, with significant production from both strains (lanes 1–4), but higher amounts in BL21 (lanes 3 and 4), and a slight reduction at higher cadmium concentrations. However, while the βMT fusion protein was again practically absent from the homogenates of JM105 cells grown in cadmium (lanes 5 and 6), amounts comparable to those obtained for GST–αMT were recovered from the BL21 host (lanes 7 and 8). These results clearly indicate that recombinant synthesis

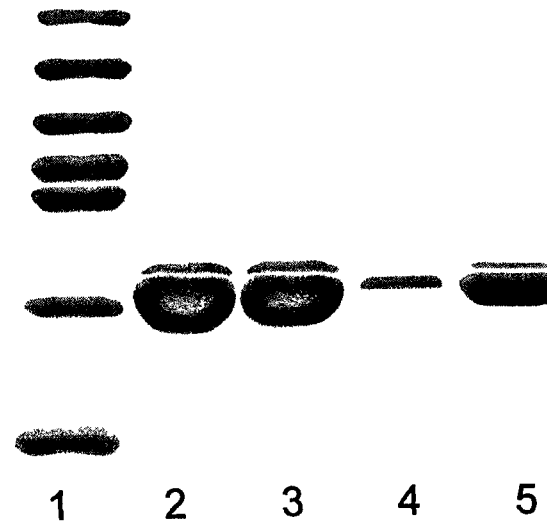

Fig. 1. SDS–PAGE, in 12.5% gels stained with Coomassie blue, of purified fusion GST–βMT domain synthesized by *E.coli* JM105 cells grown in lane 2, non-metal supplemented medium; lane 3, 300 μM Zn^{2+} supplemented medium; lane 4, 300 μM Cd^{2+} supplemented medium; lane 5, 300 μM Cu^{2+} supplemented medium. Lane 1, molecular weight markers of 97.4, 66.2, 55.0, 42.7, 40.0, 31.0 and 21.5 kDa.

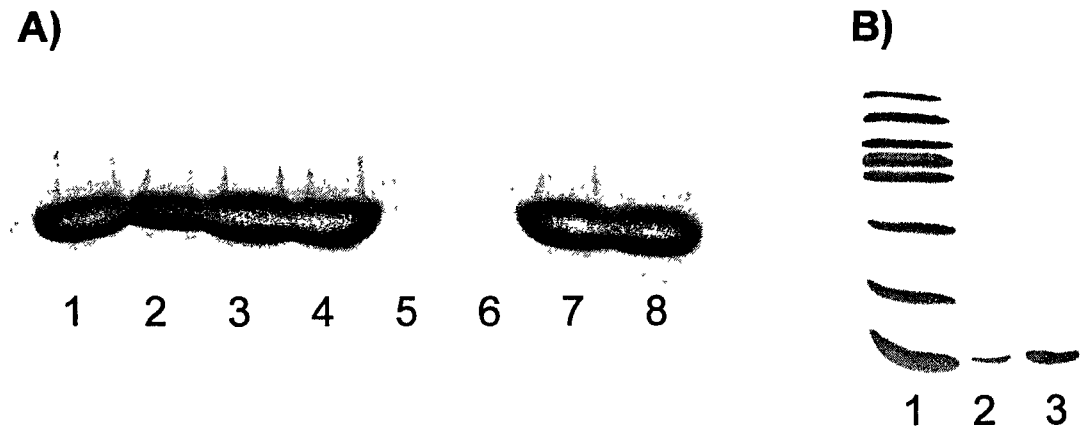

Fig. 2. (A) SDS–PAGE, in 12.5% gels stained with Coomassie blue, of purified fusion GST–MT proteins, synthesized by different *E.coli* strains, grown in cadmium media: lane 1, GST–αMT, *E.coli* JM105, 100 μM Cd^{2+}; lane 2, GST–αMT, *E.coli* JM105, 300 μM Cd^{2+}; lane 3, GST–αMT, *E.coli* BL21, 100 μM Cd^{2+}; lane 4, GST–αMT, *E.coli* BL21, 300 μM Cd^{2+}; lane 5, GST–βMT, *E.coli* JM105, 100 μM Cd^{2+}; lane 6, GST–βMT, *E.coli* JM105, 300 μM Cd^{2+}; lane 7, GST–βMT, *E.coli* BL21, 100 μM Cd^{2+}; lane 8, GST–βMT, *E.coli* BL21, 300 μM Cd^{2+}. (B) SDS–PAGE, in 15% gels stained with Coomassie blue, of Cd–βMT recovered after thrombin cleavage and FPLC chromatography from the fusion GST–βMT of two independent preparations (lanes 2 and 3). Molecular weight markers correspond to 97.4, 66 2, 55.0, 42.7, 40.0, 31.0, 21.5 and 14 4 kDa.

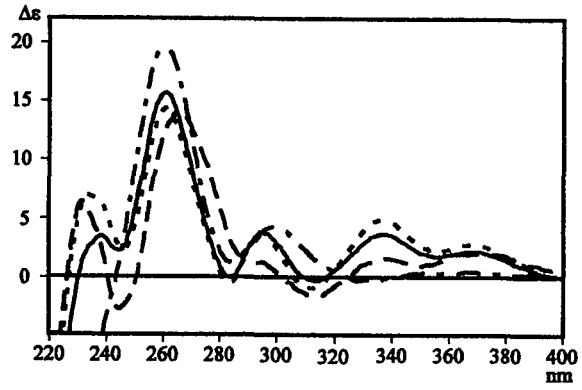

Fig. 3. Comparison of the circular dichroism spectra of the *in vivo*-synthesized Cu–βMT species (— —) with those corresponding to the Cu_6–βMT (— - —) and Cu_7–βMT (- - -) species generated *in vitro* by Zn/Cu replacement (Bofill *et al.* 1999). A computer generated spectrum corresponding to the sum of the CD spectral traces of Cu_6–βMT (25%) and Cu_7–βMT (75%) has also been included (——).

of the βMT domain in cadmium-supplemented media was essentially dependent upon the *E.coli* host strain.

Characterization of the binding abilities of the βMT domain synthesized in the presence of Cu

Cu–βMT was obtained by thrombin digestion of the GST–βMT protein recovered from *E.coli* JM105 cells grown in the presence of 500 μM Cu^{2+}. The metal content of the samples, determined by ICP-AES, was 6.3 to 6.8 Cu atoms per total sulfur content, which is consistent with the stoichiometry reported for the native mammalian βMT (Nielson and Winge, 1985). Thus, our results showed that when the βMT domain was recombinantly synthesized in the presence of copper, it was recovered as a fully loaded Cu–βMT species. Comparison of the CD spectrum with those of the Cu–βMT species generated *in vitro* by Zn/Cu replacement (Figure 3) (Bofill *et al.*, 1999) showed that the sample recovered from biosynthesis of the β domain in Cu-supplemented media contained Cu_6–βMT and Cu_7–βMT. Specifically, the CD spectral trace of the *in vivo* Cu–βMT species precisely matched the computer-generated spectrum corresponding to 75% of Cu_7–βMT plus 25% of Cu_6–βMT. This explains the Cu/protein ratios of 6.3 and 6.8 found by ICP-AES. The molecular mass of the single peak detected by ESI-MS of the Cu–βMT sample was 3599.27 (data not shown), which is consistent with the expected value of 3596.36 for the Cu_7–βMT species (apo–βMT + 7 Cu–7H). The peak corresponding to Cu_6–βMT probably remains undetectable due to the low contribution of this species (25%) and to the excessive background produced by the Tris buffer in the sample, which cannot be exhaustively dialyzed if integrity of the Cu(I) aggregates is to be preserved. Thus, our data pointed towards a major formation of a Cu_7–βMT cluster inside the cell.

Characterization of the binding abilities of the βMT domain synthesized in the presence of Cd

In order to analyze the features of the *in vivo*-structured Cd-cluster, and compare it with the Cd_3–βMT generated *in vitro* from Zn_3–βMT by Zn/Cd replacement, fusion GST–βMT was purified from total protein extracts of BL21 cells grown in 300 μM cadmium medium, and used to recover the βMT portion. Two types of culture were set up: small-scale 0.5 l cultures in Erlenmeyer flasks, grown in a New Brunswick Orbital Incubator, and large-scale 30 l cultures grown in a Biostat U (Braun Biotech) Fermentor. In both cases approximately 0.5–0.9 mg of the β peptide were recovered per litre of culture after thrombin digestion and FPLC purification. ICP-AES measurements of the cadmium versus total sulfur content invariably yielded a ratio of 1.35–1.40, in contrast to the stoichiometric relationship of 3 reported for the Cd_3–βMT species generated *in vitro*. Neither Zn nor Cu was detected in the sample. Cadmium content was consistent with a 60–63% oxidation rate indicated by the DTNB reaction for samples purified from both types of culture. So far, the results point to the presence of undermetaled cadmium species, due to partial oxidation of the thiol groups. Surprisingly, further characterization revealed a different composition of the βMT preparations obtained from the different culture conditions.

The CD spectrum of the Cd–βMT species obtained from

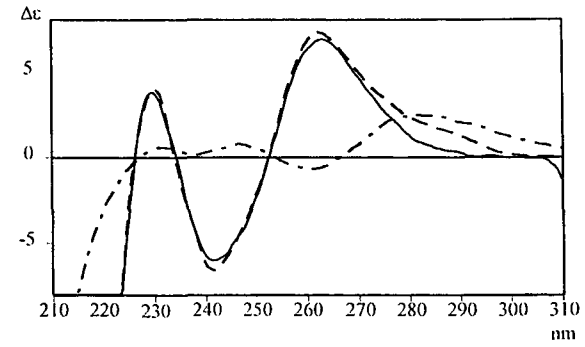

Fig. 4. Circular dichroism spectra of the *in vivo*-synthesized Cd–βMT species obtained from a 0.5 l, small-scale (— —) or a 30 l, large-scale culture (— · —). The Cd_3–βMT species generated *in vitro* by Zn/Cd replacement (Capdevila *et al.*, 1997) has also been included for comparison (——).

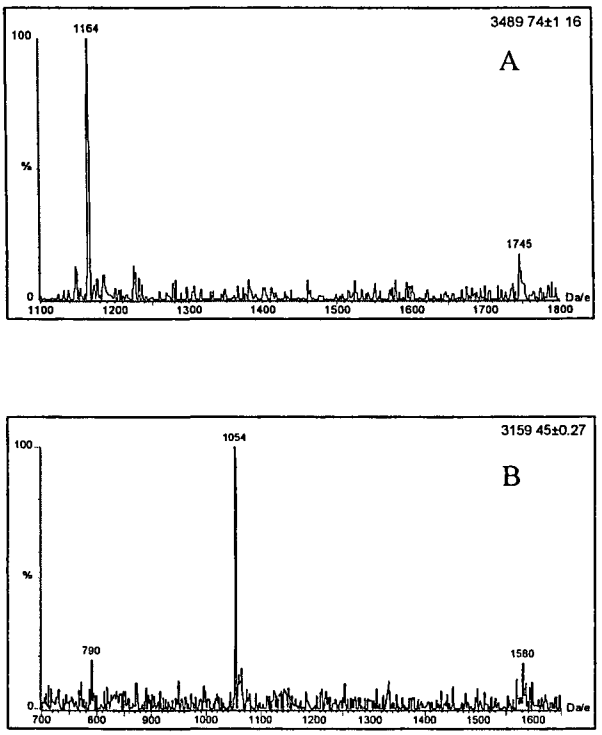

Fig. 5. ESI-MS mass spectra of the *in vivo*-synthesized Cd–βMT species. **(A)** The spectrum at pH 7 of the sample obtained from a small-scale culture (0.5 l) indicates the presence of Cd_3–βMT. **(B)** The spectrum at pH 3 of the sample obtained from a large-scale culture (30 l) shows the presence of apo-βMT. The molecular mass found in each case is given in the upper right-hand corner.

small-scale cultures paralleled that of the Cd_3–βMT species generated *in vitro* from Zn_3–βMT (Figure 4), which indicated the presence of some well-structured Cd_3–βMT clusters. The mass of these molecules was 3489.74 at pH 7.0, which coincides with the expected value of 3489.74 for Cd_3–βMT (apo-βMT + 3 Cd – 6 H) (Figure 5A). Acidification of this sample yielded an apo-form with a molecular mass of 3159.69, which agrees well with the calculated value of 3158.54 (data not shown).

In contrast, the CD features observed for the Cd–βMT species obtained from the large-scale cultures closely resembled those shown by aged Cd_3–βMT samples obtained *in vitro* and kept for several days at 4°C, indicating the absence of any Cd_3–βMT cluster in the preparation (Figure 4). Mass spectrometry at pH 7.0 did not detect either Cd_3–βMT or any definite Cd species, but acidification of the sample yielded an apo-form of molecular mass 3159.45, in agreement with the presence of whole βMT molecules in the preparation (Figure 5B), and thus indicating that the lack of well-defined metal species could not be attributed to the degradation of the β peptide.

Discussion

To date, the widely accepted preference of the βMT domain for Cu(I) over divalent ions had been inferred from *in vitro* data, and direct evidence of the ability of this fragment to form Cu or Cd aggregates *in vivo* has not been reported. Here, we describe the successful synthesis of recombinant mouse Cu–βMT and Cd–βMT, the latter only attainable in a protease-deficient *E.coli* strain, and the study of their metal-binding capacity.

In vivo, recombinant βMT binds copper to form aggregates comparable with those obtained *in vitro* by Zn/Cu replacement from Zn_3–βMT (Bofill,R., Capdevila,M., Gonzàlez-Duarte,P., Palacios,O., Cols,N., Gonzàlez-Duarte,R. and Atrian,S., manuscript submitted). The coexistence of Cu_7–βMT (75%) and Cu_6–βMT (25%) species in the samples recovered from the transformed *E.coli* cells could be due to several factors: (i) equilibrium between the two species inside the cell; (ii) a partial loss of the seventh copper ion during sample manipulation; or (iii) the restrictive source of Cu(I) ions. The formation of the Cu_7–βMT cluster *in vivo*, as revealed by ESI-MS and CD spectroscopy, is consistent with previous *in vitro* copper-coordination data (Nielson and Winge, 1985), and reinforces the hypothesis of the primeval copper affinity of the β domain.

In contrast, Cd–βMT aggregates were recovered only in special conditions: in a protease-deficient *E.coli* strain, BL21, and expressed as a fusion protein, GST-tailed. The almost complete absence of Cd–βMT–GST fusion protein in JM105 cells (Figures 1 and 2) fully agrees with reported results (Sewell *et al.*, 1995; Kurasaki *et al.*, 1996, 1997). In addition, the stability of the Cd–βMT aggregates was found to be dependent upon culture conditions. On the one hand, preparations obtained from small-scale cultures were a mixture of approximately one third Cd_3–βMT, with identical structure to that generated *in vitro* through Zn/Cd replacement (Capdevila *et al.*, 1997), and two thirds of fully oxidized protein, devoid of Cd(II) ions. On the other, large-scale cultures did not produce the Cd_3–βMT species, but probably less structured and partially oxidized Cd–βMT aggregates. Our data are also in accordance with several *in vitro* βMT cadmium-binding studies, showing that the apo-βMT peptide is not prone to form *de novo* stable Cd_3 clusters (Nielson and Winge, 1985; Kull *et al.*, 1985; Stillman *et al.*, 1987).

It is tempting to speculate on the lack of βMT recovery from cadmium cultures. The finding that a protease-deficient host could yield high amounts of the β domain argues in favour of a post-translational proteolytic degradation of βMT. Indeed, the evidence that βMT mRNA is present in transformed *E.coli* JM105 cells, which never accumulates the recombinant peptide, was reported by Kurasaki *et al.* (1996). Furthermore, the low affinity of the β peptide towards cadmium would impair correct folding or lead to conformational changes and

so favour its vulnerability to proteolysis Finally, it had been shown that hydrolysis of thioamide peptides by carboxypeptidase A increases 240–970% in the cadmium-substituted enzyme (Bond *et al*, 1986) This is consistent with the hypothesis that cadmium, a thiophilic metal, increases the positive character of the carbonyl carbon and facilitates the nucleophilic attack of substrates by the proteolytic metalloenzymes

From the present data, functional and evolutionary implications could also be drawn If primeval βMT forms were selected on the basis of their contribution to homeostasis of physiological metals, mainly Cu and Zn, this particular feature would have been retained by the present mammalian β domain, although probably blurred by its interaction with the α counterpart This has previously been shown for Zn (Capdevila *et al*, 1997), and is now confirmed for Cu As a further evolutionary step, the duplication of the βMT domain may have led to a derived αMT peptide, which conferred upon the organisms the capacity to respond to newly encountered toxic metals, such as cadmium This would account for the poor *in vivo* reactivity of βMT towards cadmium, as also described in this work, mainly if compared with its affinity for metals associated with life processes, such as Cu or Zn Further in-depth investigation of the interaction mechanisms between different metal ions and the βMT thiol groups should be now facilitated by the availability of functional recombinant βMT peptide

Acknowledgements

This work was supported by the Spanish Ministerio de Educación y Ciencia (grants PB94-0695 and PB96-0225) and the Departament de Medi Ambient de la Generalitat de Catalunya We thank the Serveis Científico-Tècnics, Universitat de Barcelona, for allocating instrument time to this research M C is indebted to the Fundacion Caja de Madrid for a post doctoral scholarship and R B to the Comissionat per a Universitats i Recerca de la Generalitat de Catalunya (CIRIT) for pre doctoral scholarships We also thank R Rycroft for revising the English version of this manuscript

References

Bernhard,W R , Vasak,M and Kagi,H R (1986) *Biochemistry*, **25**, 1975–1980
Birchmeier,W and Christen,P (1971) *FEBS Lett* , **18**, 208–213
Bofill,R , Palacios,O , Capdevila,M , Cols,N , Gonzalez-Duarte,R , Atrian,S and Gonzalez Duarte,P (1999) *J Inorg Biochem* , in press
Bond,M D , Holmquist,B and Vallee,B L (1986) *J Inorg Biochem* , **28**, 97–105
Capdevila,M , Cols,N , Romero-Isart,N , Gonzalez-Duarte,R , Atrian,S and González Duarte,P (1997) *Cellular and Molecular Life Sciences* (formerly *Experientia*), **53**, 681–688
Chernaik,M L and Huang,P C (1991) *Proc Natl Acad Sci USA*, **88**, 3024–3028
Cols N , Romero Isart N Capdevila,M , Oliva,B Gonzalez-Duarte,P , González-Duarte,R and Atrian,S (1997) *J Inorg Biochem* , **68**, 157–166
Furey,W F , Robbins,A H , Clancy,L L , Winge D R , Wang,B C and Stout,C D (1986) *Science*, **231**, 704–710
Kagi,J H R (1993) In Suzuki,K T , Imura N and Kimura,M (eds) *Metallothionein III Biological Roles and Implications* Birkhauser Verlag, Basel, pp 29–55
Kull F J , Reed,H F , Elgre,T E , Ciardelli,T L , Wilcox,D E (1990) *J Amer Chem Soc* , **112**, 2291–2298
Kurasaki,M , Emoto,T , Arias,A L , Okabe,M , Yamasaki,F , Oikawa S and Kojima,Y (1996) *Protein Engng* **9**, 1173–1180
Kurasaki M , Yamaguchi R Arias A , Okabe M and Kojima,Y (1997) *Protein Engng* **10** 413–416
Li H and Otvos J D (1996) *Biochemistry*, **35** 13929–13936
McCormick C C and Lin L -Y (1991) *Methods Enzymol* , **205** 71–78
Narula S S , Brouwer,M Hua Y and Armitage,I M (1995) *Biochemistry* **34** 620–631
Nemer,M , Wilkinson D G Travaglini E C , Sternberg E J and Butt T R (1985) *Proc Natl Acad Sci USA* **82** 4992–4994
Nielson K B and Winge D R (1984) *J Biol Chem* **259** 4941–4946
Nielson,K B and Winge,D R (1985) *J Biol Chem* , **260**, 8698–8701
Nielson,K B , Atkin,C L and Winge,D R (1985) *J Biol Chem* , **260**, 5342–5350
Okada,Y , Ohta,N , Yagyu,M , Min,K -S , Onosaka,S and Tanaka,K (1985) *FEBS Lett* , **183**, 375–378
Okada,Y , Ohta,N , Iguchi,S , Tsuda,Y , Sasaki,H , Kitagawa,T , Yagyu,M , Min,K -S , Onosaka,S and Tanaka,K (1986) *Chem Pharm Bull* , **34**, 986–998
Otvos,J D and Armitage,I M (1980) *Proc Natl Acad Sci USA*, **77**, 7094–7098
Peterson,C W , Narula,S S and Armitage,I M (1996) *FEBS Lett* , **379**, 85–93
Sewell,A K , Jensen,L T , Erickson,J C , Palmiter,R D and Winge,D R (1995) *Biochemistry*, **34**, 4740–4747
Shi,J , Lindsay,W P , Huckle,J W , Morby,A P and Robison,N J (1992) *FEBS Lett* , **303**, 159–163
Stillman,M J , Cai,W and Zelazowski,A J (1987) *J Biol Chem* , **262**, 4538–4548
Tommey,A M , Shi,J , Lindsay,W P , Urwin,P E and Robison,N J (1991) *FEBS Lett* , **292**, 48–52
Wang,Y J , Mackay,E A , Zerbe,O , Hess,D , Hunziker,P E , Vasák,M and Kagi,J (1995) *Biochemistry*, **34**, 7460–7467
Winge,D R , Nielson,K B , Gray,W R and Hamer,D H (1985) *J Biol Chem* , **260**, 14464–14470
Winge,D R (1991) *Methods Enzymol* , **205**, 458–469
Xiong,Y and Ru,B (1997) *J Biochem* , **121**, 1102–1106

Received April 28 1998 revised November 23, 1998, accepted December 11, 1998

Article 3

R. Bofill, M. Capdevila, N. Cols, S. Atrian, P. Gonzàlez-Duarte.

Zn(II) is required for the *in vivo* and *in vitro* folding of mouse Cu-metallothionein in two domains.

J. Biol. Inorg. Chem., **2001**, 000.

Zn(II) is required for the *in vivo* and *in vitro* folding of mouse Cu-metallothionein in two domains

Roger Bofill[1], Mercè Capdevila[1], Neus Cols[2], Sílvia Atrian[2], Pilar Gonzàlez-Duarte[1]✉

✉ To whom correspondence should be sent

[1] Departament de Química, Facultat de Ciències, Universitat Autònoma de Barcelona, E-08193 Bellaterra, Barcelona, Spain

Tel.: + 34 935 811 363; Fax: + 34 935 813 101

e-mail: Pilar.Gonzalez.Duarte@uab.es

[2] Departament de Genètica, Facultat de Biologia, Universitat de Barcelona, Av. Diagonal 645, E-08071 Barcelona, Spain

Abbreviations CD, circular dichroism; ESI-MS, electrospray ionisation mass spectrometry; ICP-AES, inductively coupled plasma-atomic emission spectroscopy; MT, metallothionein; UV-Vis, ultraviolet-visible electronic absorption

Abstract We postulate that Zn(II) is a keystone in the structure of physiological mouse Cu-MT 1. Only when Zn(II) is co-ordinated does the structure of the *in vivo*- and *in vitro*-conformed Cu-MT species consist of two additive domains. Therefore, the functionally active forms of the mammalian Cu-MT may rely upon a two-domain structure. The *in vitro* behaviour of the whole protein is deduced from the Cu titration of the apo and Zn-containing forms and compared with that of the independent fragments using CD, UV-Vis, ESI-MS and ICP-AES. We propose the formation of the following Cu,Zn-MT species during Zn/Cu replacement in Zn_7-MT: $(Zn_4)^{\alpha}(Cu_4Zn_1)^{\beta}$–MT, $(Cu_3Zn_2)^{\alpha}(Cu_4Zn_1)^{\beta}$–MT and $(Cu_4Zn_1)^{\alpha}(Cu_6)^{\beta}$–MT. The cooperative formation of $(Cu_3Zn_2)^{\alpha}(Cu_4Zn_1)^{\beta}$–MT from $(Zn_4)^{\alpha}(Cu_4Zn_1)^{\beta}$–MT indicates that the preference of Cu(I) for binding to the β domain is only partial and not absolute, as otherwise accepted. Homometallic Cu-MT species have been obtained either from the apoform of MT or from Zn_7-MT after total replacement of zinc. In these species copper distribution cannot be inferred from the sum of the independent α and β fragments. The *in vivo* synthesis of the entire MT in Cu-supplemented media has afforded Cu_7Zn_3-MT [$(Cu_3Zn_2)^{\alpha}(Cu_4Zn_1)^{\beta}$–MT], while that of αMT has rendered a mixture of Cu_4Zn_1-αMT (40%), Cu_5Zn_1-αMT (20%) and Cu_7-αMT (40%). In the case of βMT a mixture of Cu_6-βMT (25%) and Cu_7-βMT (75%) was recovered [1]. These species correspond to some of those conformed *in vitro* and confirm that Zn(II) is essential for the *in vivo* folding of Cu-MT in a Cu-rich environment. A final significant issue is that common procedures used to obtain mammalian Cu_6-βMT from native sources may not be adequate.

Key words Copper-metallothionein · Copper and zinc-metallothionein · Recombinant metallothionein · Copper-α domain · *In vivo* Cu-metallothionein

Introduction

Metallothioneins (MT) are ubiquitous, low-molecular-weight, cysteine-rich proteins characterised by an exceptional heavy metal binding capacity. They are thought to be involved in Cu and Zn homeostasis and in the protection against damage from toxic metal ions, free radicals and other electrophilic agents [2, 3]. Mammalian MT consist in two domains, α and β, which contain 11 and 9 co-ordinating Cys, respectively [4]. Copper mammalian MT have been extensively studied, mainly *in vitro*, yielding a variety of results on the Cu-binding stoichiometry of the α [5, 6, 7, 8, 9] and β domains [5-8, 10, 11] or the entire MT [8, 12, 13, 14, 15, 16, 17, 18, 19]. Up to the present, it has been widely accepted that both domains behave independently [11] and that Cu(I) binds preferentially to the β domain [5, 10-12].

Synthesis of the individual domains of MT and comparison of their behaviour with that of the whole protein may increase the present, still enigmatic, understanding of the role of MT in living organisms [20]. For this purpose we have used the recombinant DNA approach, which allowed us to obtain Zn_7-MT as well as its two constitutive Zn_4-αMT and Zn_3-βMT fragments [21, 22], the latter for the first time. This synthetic procedure, which renders high purity preparations, has enabled us to extend previous knowledge on the coordinative features of these proteins both under *in vitro* [21, 22, 23, 24] and *in vivo* [1] conditions.

One main feature observed in native MT synthesised by mammals fed or injected with metals such as Cu or Cd is that the corresponding metal clusters also contain Zn(II) ions [4, 8, 25, 26, 27, 28, 29, 30]. Zinc is a key structural or catalytic component of a large number of proteins [31], including MTF-1, the transcription factor regulating the mammalian MT gene expression, whose DNA binding ability is dependent on Zn-activation [32]. The relation between the zinc clusters of MT and its functional potential, as well as the possible domain interactions has been the object of intensive studies [33]. Thus, the presence of Zn(II) in Cu-MT species should be also analysed from the perspective of its significance in physiological-stable MT forms.

In this article we report our results on the Cu(I) binding abilities of recombinant mouse MT and its α fragment. These, together with those corresponding to the β fragment [1, 24], illustrate the role of Zn(II) as a keystone in the structure of MT and its significance in the dependence/independence between domains. Furthermore, the stoichiometry of the species formed along the titration of Zn_7-MT with Cu(I) shows that this ion has an unclear preferential binding for the β domain. In order to corroborate the structural significance of Zn(II) in Cu-MT species in physiological conditions, we undertook the recombinant expression of mouse MT 1 and its α fragment in copper-supplemented media. Data for the β fragment have already been reported [1]. All the results obtained *in vivo* are in good concordance with those obtained *in vitro*. The former show that the entire MT, even in Cu-saturation conditions, does not form fully Cu-loaded aggregates and, conversely, the unique MT species recovered contains Zn(II) ions in both α and β domains.

Materials and methods

Protein Preparation and Characterisation. Fermentator-scale cultures, purification of the GST-MT fusion proteins and recovery and analysis of the recombinant mouse Zn_7-MT and the Zn_4-αMT 1 domain were performed as previously described [21, 22]. Accordingly, the Zn_7-MT and Zn_4-αMT species were obtained in Tris-HCl 50 mM buffer, pH 7. Protein solutions had a final concentration of 127 μM (α fragment) and 54.8 μM (MT). These were diluted to a final concentration of 20 μM (α fragment) or 10 μM (MT) with Milli Q-purified and Ar-degased water, and were titrated with freshly prepared solutions of $[Cu(CH_3CN)_4]^+$ in CH_3CN/H_2O at 25 °C.

The apoproteins were prepared by acidification of the recombinant material with HCl 10^{-2} M until pH 3. At pH values lower than 3.5 the Zn_4-αMT and Zn_7-MT species are entirely demetalated, according to their respective CD spectra. In contrast, Cu(I) remains bound to S-Cys at pH down to 1.5.

Recombinant expression, purification and metal content analysis of αMT and the entire MT as Cu-complexes were carried out as previously described for βMT [1], using the same expression vectors as for the Zn-complexes [21, 22].

Metal Solutions. Glassware and solutions used in metal ion binding studies were prepared as described [22]. Due to the known sensitivity of Cu(I) to both oxidation and disproportionation, the solutions of Cu(I) were prepared from the stable $[Cu(CH_3CN)_4]ClO_4$ complex [34], in 30% (v/v) CH_3CN/H_2O. Concentration of Cu stock solutions were quantified and the absence of detectable Cu^{2+} in these solutions, before and after use as a titrating agent, was confirmed as already described [24]. The concentration of the Cu(I) solutions used for titration was in the range 10^{-2} - 10^{-3} M.

Metal Ion Binding Reactions. Metal binding experiments were carried out by sequentially adding molar-ratio aliquots of concentrated Cu(I) stock solutions to a single solution of either Zn_4-αMT, apo-αMT, Zn_7-MT or apo-MT. For each addition, the

protein sample was allowed to react with the metal ion under thermodynamic conditions [24]. In the case of the titration of Zn_4-αMT with Cu(I) at pH 7 each molar-ratio aliquot of Cu(I) was added to the Ar-saturated solution every 24 hours because of the slow stabilisation of the species formed. Absorption studies were conducted in parallel with CD studies.

All manipulations involving the metal and protein solutions were performed in Ar atmosphere, and titrations were carried out at least in duplicate to assure the reproducibility of each single point.

The pH (7 or 3) for all experiments remained constant throughout without addition of buffers and the temperature was kept constant at 25 °C. The electronic absorption and CD measurements were performed and corrected as already described [24].

Chelex-100 experiments. The possibility that Zn(II) remained bound to the protein in the Cu(I)-αMT and Cu(I)-MT species formed in the respective titrations of Zn_4-αMT and Zn_7-MT at pH 7 was considered. In order to determine the zinc content in the Cu,Zn species, a second titration was carried out until the formation of the suspected mixed-metal species. Following this, a small quantity of Chelex-100 was added to the solution as already described [22]. The sulfur, zinc and copper contents of the supernatant and of the solutions obtained after treatment of the resin with 2 M HNO_3 were analysed. Total sulfur, zinc and copper contents were measured by inductively coupled plasma-atomic emission spectroscopy (ICP-AES) [35] using a Thermo Jarrell Ash, Polyscan 61E measuring at 182.040 nm (S), 213.856 nm (Zn) and 324.754 nm (Cu). In all cases, it was verified that the CD and UV-Vis spectra corresponding to the mixed-metal species remained unchanged after the treatment with Chelex-100.

Molecular mass determination. The molecular masses of all the Cu and Cu,Zn-containing species obtained *in vitro* and *in vivo* were determined by electrospray ionisation mass spectrometry (ESI-MS) on a Fisons Platform II Instrument (VG

Biothech) equipped with the Mass Lynx software provided by the manufacturer, calibrated using horse heart myoglobin (0.1 mg/ml). Different sets of conditions were required depending on the sample. For the Cu-MT species obtained *in vitro* at pH 7, 10 µl of protein solution were injected through a PEEK (polyether heteroketone) column (1m x 0.007 inch i.d.) at 30 µl/min; source temperature, 180 °C; capillary counter electrode voltage, 4500 V; lens counter electrode voltage, 500 V; cone potential, 50 V; *m/z* range, 750-1900; scanning rate, 2.5 s/scan; interscan delay, 0.3 s. The liquid carrier was a mixture of 3mM ammonium formate / ammonia (pH 7), 1 µM mercaptoethanol (eluent A) and methanol (eluent B) at the following A:B ratios: 95:5 (0-1 min), 50:50 (min 5), 95:5 (min 6). The molecular masses of the Cu-αMT species obtained *in vitro* at pH 7, as well as those of the *in vivo*-synthesised Cu-MT and Cu-αMT species, were determined as described above except for the following conditions: lens counter electrode voltage, 1000V; A:B ratios of the liquid carrier, 95:5 (0-3 min), 50:50 (min 6), 95:5 (min 7). For the Cu-MT and Cu-αMT samples at pH 3, 10 µl of protein solution were injected through a PEEK column (1m x 0.007 inch i.d.) at 20 µl/min; source temperature, 60 °C; capillary counter electrode voltage, 3500 V; lens counter electrode voltage, 500 V; cone potential, 60 V; *m/z* range, 750-1900; scanning rate, 2.5 s/scan; interscan delay, 0.3 s. The liquid carrier was a 50:50 mixture of acetonitrile and formic acid (pH 3), 1 µM mercaptoethanol. The PEEK column was used to avoid the masking effect of the Tris buffer, while mercaptoethanol was added to avoid the oxidation of Cu(I) ions. Masses for the holo-species were calculated according to the literature [36]. Determination of the exact stoichiometry of Cu_xZn_y species from ESI-MS data is hindered by the closeness of the atomic weights of Cu(I) and Zn(II). In such cases, a combined evidence based on complementary data (Chelex-100 experiments, UV-Vis and CD, as well as ESI-MS for related species) facilitates a final decision.

Throughout this paper we refer to the mol equivalents of Cu(I) added in terms of "x Cu(I)" to stand for "x mol equivalents of Cu(I)" or "a molar ratio Cu(I) : protein of x".

Results

Cu-MT and Cu-αMT species have been identified from saturation of the chiral intensity and changes in the CD and UV-Vis spectra as increasing amounts of Cu(I) are added to the protein solution. In most cases the stoichiometry of the species formed has been confirmed by ESI-MS. Determination of the stoichiometry of Cu,Zn mixed-metal species has required additional Chelex-100 experiments coupled to ICP-AES data.

The analysis of the behaviour of the recombinant proteins at pH 7 towards Cu(I) requires knowledge of the role played by the Zn atoms. Thus, the interpretation of the spectral changes accompanying the addition of Cu(I) to the Zn-metalated proteins must take into account the spectral signals due to the SCys→Zn^{2+} LMCT bands, which can overlap with the new bands related to copper-thiolate interactions. Titration of the apoproteins with Cu(I) provides information on the signals corresponding to the Cu-SCys chromophores and allows evaluation of the masking effects due to the Zn-SCys co-ordination at pH 7.

Figures 1, 2, 4 and 5 show the CD spectra recorded during the titration of recombinant apo-αMT (pH 3), Zn_4-αMT (pH 7), apo-MT (pH 3) and Zn_7-MT (pH 7) with Cu(I), respectively. The corresponding electronic absorption spectra and difference spectra of the latter are provided as Supplementary Material. As expected, the CD spectra of the apo-αMT (Fig. 1, line 0) and apo-MT species (Fig. 4, line 0) have no significant signals above 250 nm, while those of Zn_4-αMT (Fig. 2, line 0) and Zn_7-MT (Fig. 5, line 0) show their characteristic biphasic CD features [21, 22].

Binding abilities of the recombinant mouse αMT fragment in the presence of Cu(I) ions

Cu(I) binding abilities of apo-αMT at pH 3

From 0 to 3 mol equivalents of Cu(I) added to apo-αMT at pH 3, CD spectra develop isodichroically to form two derivative-like envelopes with positive bands at

260.5 and 310 nm and a negative superimposed band at 288.5 nm. Moreover, a positive band appears at 354 nm, Fig. 1. The absorption spectra show a linear increase of a band centred at 260-270 nm, while the difference spectra are coincidental and present three contributions at 235, 260-270 and 300 nm approx. All these spectral data are indicative of the cooperative formation of a Cu_3-αMT species from apo-αMT. While the CD spectra do not change significantly from 3 to 5 mol equivalents, the addition of two more Cu(I) equivalents, from 5 to 7, provokes a blue shift of the 260(+) nm band. The UV-Vis difference spectra also show a blue shift of the contribution at 265 nm from 3 to 7 Cu(I) added while two new contributions appear at 283 and 335 nm at more than 6 Cu(I) added. All these features indicate that Cu_3-αMT evolves to a Cu_5-αMT species without significant alteration of the structure, and that Cu_5-αMT converts to a Cu_7-αMT species with different Cu(I)-SCys co-ordination geometries from the former. The profile of the CD spectra smoothes from 7 to 9 Cu(I) added, and at more than 9 Cu(I) added the CD and absorption spectra do not change significantly, while the UV-Vis difference spectra only show the contributions due to the titrating agent. This suggests that Cu(I) does not bind to the α fragment at more than 9 mol equivalents added.

Unfortunately, no species of the Cu-αMT samples have been detected by ESI-MS at pH 3, in agreement with the common difficulties associated with the artefactual clustering and oxidation either of Cu(I) to Cu(II) ions or of thiolate to difulfide bonds in homometallic Cu-containing MT species [37].

Cu(I) binding abilities of Zn_4-αMT at pH 7

The CD spectra recorded during the addition of the first 3 Cu(I) to Zn_4-αMT at pH 7, Fig. 2, show a red shift of the characteristic band of Zn_4-αMT, indicating a partial Zn/Cu replacement. The isodichroicity observed together with the coincidental UV-Vis difference spectra account for a cooperative formation of a Cu_3Zn_x-αMT species ($x < 4$). As a means of determining x, a parallel titration was carried out with addition of Chelex-100 after incorporation of the first three Cu(I) ions in order to bind the displaced Zn(II) ions [22] (data not shown). Analytical results indicated that the chelating resin

sequestered 2 Zn and that the protein maintained 3 Cu and 2 Zn atoms co-ordinated. Furthermore, ESI-MS measurements performed on aliquots of a parallel titration showed the unique presence of Zn_4-αMT and Cu_3Zn_2-αMT after 2 Cu(I) added and a predominant Cu_3Zn_2-αMT species after 3 Cu(I) added (Table 1). Therefore, a stoichiometric ratio of Cu_3Zn_2-αMT for the species formed cooperatively in the first stage of the titration is postulated. The next two Cu(I) equivalents, from 3 to 5, provoke a red shift of the derivative-like envelope; the shift also being observed in the UV-Vis difference spectra. These data indicate the partial replacement of Zn by Cu atoms, which accounts for the non-cooperative conversion of Cu_3Zn_2-αMT into Cu_5Zn_1-αMT passing through a Cu_4Zn_x-αMT (x = 1, 2) intermediate. The formation of Cu_5Zn_1-αMT can be postulated on the basis of the Zn/Cu replacement observed during the next stage of the titration and its detection by ESI-MS in a parallel titration after 5 Cu(I) added (Table 1). In order to determine whether x is 1 or 2 in Cu_4Zn_x-αMT, ESI-MS measurements were performed, and the presence of a predominant Cu_4Zn_1-αMT species after 4 Cu(I) added was determined (Table 1). From 5 to 7 Cu(I) equivalents the CD and UV-Vis difference bands red shift. This can be explained in terms of a further replacement of Zn by Cu atoms, which causes Cu_5Zn_1-αMT to turn into Cu_7-αMT. Addition of copper from 7 to 9 equivalents results again in a red shift of the CD bands with a concomitant decrease in intensity of the positive band, which causes the disappearance of the derivative-like envelope. The absorption spectra decrease in intensity, indicating the loss of specific Cu-S cromophores formed during the previous stages. All these spectral data account for the formation of a Cu_9-αMT species with different Cu-S co-ordination environments and lower degree of folding than those in Cu_7-αMT. Unfortunately, it has not been possible to detect the Cu_7-αMT or the Cu_9-αMT species in solution by ESI-MS. At more than 9 Cu(I) added the CD spectra do not change significantly and the UV-Vis difference spectra only show the contributions due to the titrating agent. These data suggest that at pH 7 Cu(I) does not bind to the α fragment at more than 9 Cu(I) added, exactly as it occurred at pH 3.

Overall, the stoichiometry of the species formed along the titration of either apo-αMT at pH 3 or Zn_4-αMT at pH 7 with Cu(I) and the corresponding reaction pathways are given in Fig. 3. As expected, these are highly dependable on the nature of the initial species. Thus, in the first stages of the titrations Cu_3-αMT and Cu_5-αMT, with closely related structures, are formed *de novo* from the apoform of αMT, while Cu_3Zn_2-αMT, Cu_4Zn_1-αMT and Cu_5Zn_1-αMT are obtained during Zn/Cu replacement from Zn_4-αMT. From this point homometallic species of the same stoichiometry, Cu_7-αMT and Cu_9-αMT, are formed in both titrations. However, according to their CD features, in each case the two species with the same stoichiometry have different structures, which should be regarded as a consequence of the different reaction pathways followed for their formation.

Binding abilities of the recombinant entire mouse MT in the presence of Cu(I) ions

Cu(I) binding abilities of apo-MT at pH 3

From 0 to 6 mol equivalents of Cu(I) added to apo-MT at pH 3, four dichroic bands develop, Fig. 4, and the UV-Vis absorption centred at approx. 265 nm increases linearly. The UV-Vis difference spectra show the cooperative formation of a Cu_6-MT species. Furthermore, ESI-MS measurements of aliquots from a parallel titration showed the only presence of apo-MT and Cu_6-MT in a similar concentration ratio after 3 Cu(I) added and a predominant Cu_6-MT species after 6 Cu(I) added (Table 1). In the second stage of the titration, from 6 to 9 Cu(I) equivalents, the CD bands remain almost invariant. The UV-Vis difference spectra indicate that the Cu_6-MT species evolves cooperatively to form Cu_9-MT, which according to CD data has a similar structure to that of the former species. CD bands evolve isodichroically from 9 to 12 Cu(I) equivalents and the UV-Vis difference spectra show a decrease in the absorbance below 280 nm from 9 to 11 Cu(I) equivalents added. The twelfth Cu(I) causes a different effect. All these spectral data indicate that Cu_9-MT evolves first to a Cu_{11}-MT species and then to a Cu_{12}-MT species. Addition from 12 to 15 Cu(I) results in a blue shift of the

main CD band, indicating that Cu_{12}-MT evolves to a Cu_{15}-MT species. At more than 15 Cu(I) added spectral data indicate that at pH 3 Cu(I) does not bind to MT. As already noted, despite many attempts, it has not been possible to detect the homometallic Cu_9-MT, Cu_{11}-MT, Cu_{12}-MT and Cu_{15}-MT species in solution by ESI-MS.

Cu(I) binding abilities of Zn_7-MT at pH 7

The addition of Cu(I) to Zn_7-MT (Fig. 5) causes an increase of its characteristic CD fingerprint and the appearance of a shoulder at *ca.* 260 nm. Besides, two weaker bands with a derivative-like envelope gradually intensify through two isodichroic points. The UV-Vis difference spectra indicate a cooperative effect in the binding of the first 4 Cu(I) ions, which give rise to a Cu_4Zn_x-MT species. As already indicated, addition of Chelex-100 [22] in a parallel titration after incorporation of the first four Cu(I) ions allowed determination of x (data not shown). ICP-AES showed that at this point 2 Zn were in the solution while the protein maintained 4 Cu and 5 Zn co-ordinated. The presence of a Cu_4Zn_5-MT species after the addition of 4 Cu(I) equivalents to Zn_7-MT at pH 7 has also been confirmed by ESI-MS (Table 1). The next three Cu(I) equivalents, from 4 to 7, cause an isodichroical red shift of the main CD band. These CD data together with the UV-Vis data indicate that Cu_4Zn_5-MT turns cooperatively into a Cu_7Zn_x-MT species ($x < 5$). ESI-MS measurements indicated the presence of a predominant Cu_7Zn_3-MT species (Table 1). Moreover, the cooperativity of this stage has also been confirmed by ESI-MS, as an aliquot withdrawn after 6 Cu(I) added showed the presence of a mixture of the Cu_7Zn_3-MT and Cu_4Zn_5-MT species, the former being predominant (Table 1). From 7 to 10 Cu(I) equivalents, the dichroic intensities increase and reach their maximum value for 10 Cu(I) added, while new and weak bands appear, through isodichroic points. The UV-Vis difference absorption spectra evolve identically as in the previous stages. Hence, this third stage of the titration consists of the cooperative formation of a $Cu_{10}Zn_x$-MT species ($x < 3$). According to ESI-MS data, $x = 1$. This technique also confirmed the cooperative formation of $Cu_{10}Zn_1$-MT, as an aliquot withdrawn after 9 Cu(I) added showed the

major presence of Cu_7Zn_3-MT and $Cu_{10}Zn_1$-MT (Table 1). The addition of the next two Cu(I) equivalents, from 10 to 12, causes a decrease in the intensities of the two principal positive dichroic bands together with a red shift of the first one, through isodichroic points. The UV-Vis difference spectra evidence a red shift of the initial absorption band and the appearance of a new absorption. These spectral data account for the transformation of $Cu_{10}Zn_1$-MT into Cu_{12}-MT, whose formation has been corroborated by ESI-MS (Table 1). During the next stage, from 12 to 15 Cu(I) added, the main CD band decreases in intensity and blue shifts while a new positive band appears. The UV-Vis difference spectra show a decrease in intensity and a red shift of the absorptions. These spectral data account for the evolution from Cu_{12}-MT to a Cu_{15}-MT species, which includes different copper co-ordination environments than those present in Cu_{12}-MT. Moreover, the Cu_{15}-MT species has also been detected by ESI-MS (Table 1). At more than 15 Cu(I) equivalents added the intensity of the low energy CD band decreases, while the UV-Vis difference spectra indicate that at pH 7 Cu(I) does not bind to MT. These data suggest that the structure of the Cu_{15}-MT species is slightly modified by the addition of extra Cu(I) although these ions do not bind covalently to the protein.

Summarising (Fig. 6), titration of either apo-MT at pH 3 or Zn_7-MT at pH 7 with Cu(I) leads to the formation of different species in the first stages of the titrations depending on the initial species: Cu_6-MT, Cu_9-MT and Cu_{11}-MT are obtained from apo-MT, while Cu_4Zn_5-MT, Cu_7Zn_3-MT and $Cu_{10}Zn_1$-MT are formed from Zn_7-MT. In the last stages, homometallic species with the same stoichiometry but a different structure, Cu_{12}-MT and Cu_{15}-MT, are found depending on the binding pathway followed for their formation, as occurred with the homometallic Cu species of the α fragment.

***In vivo* copper binding abilities of the recombinant entire mouse MT and its α fragment**

ICP-AES and ESI-MS data show that the synthesis of recombinant entire mouse MT in Cu-supplemented media affords a single mixed-metal species, while in the case of the α fragment a mixture of species is obtained.

After the expression of the entire MT, a single Cu_7Zn_3-MT species has been found by ESI-MS, which is in concordance with ICP-AES data (Table 2). Moreover, the similarity between the CD spectra corresponding to the *in vivo*-synthesised Cu-MT and to the Cu_7Zn_3-MT species obtained *in vitro* (Fig. 7A) indicates that both metal aggregates have a very close structure.

With regard to the synthesis of αMT, ESI-MS data indicate the presence of a major Cu_4Zn_1-αMT and a minor Cu_5Zn_1-αMT species, but these data do not agree with the 4.5 Cu: 0.5 Zn ratio observed by ICP-AES. The average ratio found of 0.5 Zn per molecule gave us an indication that an homometallic Cu-αMT species, undetected by ESI-MS, could be present in the mixture. This was further confirmed as the CD features of *in vivo*-synthesised Cu-αMT resemble more those of Cu_7-αMT than those of Cu_4Zn_1-αMT and Cu_5Zn_1-αMT (Fig. 7B). The presence of Cu_7-αMT in the mixture of *in vivo*-synthesised Cu-αMT is compatible with the fact that the former is not observed by ESI-MS, as the homometallic Cu-αMT species (Fig. 3) have shown to be elusive to ESI-MS under varied experimental conditions. Overall, the 4.5 Cu: 0.5 Zn ratio together with the CD and ESI-MS data suggest a mixture of 40% Cu_4Zn_1-αMT, 20% Cu_5Zn_1-αMT and 40% Cu_7-αMT as a result of the folding of the α fragment in an intracellular Cu-supplemented environment. This ratio affords the best fit to our experimental data, as shown in Fig. 7C.

Discussion

A thorough analysis of our CD, UV-Vis, ICP-AES and ESI-MS data has led us to propose definite stoichiometries and reaction pathways for the species formed during the titrations of Zn_4-αMT and Zn_7-MT at pH 7 and pH 3 (Fig. 3 and 6). Apparently it could be considered that these results only contribute to enlarge the diversity in the number and the stoichiometries already reported for mammalian copper MT species [5-9, 12-19]. Moreover, the scarcity of established correlations between the stereochemistry around copper in copper thiolates and the corresponding absorption energies hinders us from assigning a specific type of co-ordination for the copper centres in the species reported in this study. Despite these drawbacks, a deeper insight into the results obtained, including those we reported for the titration of the β fragment [24], enables us to go further in the analysis of the behaviour of recombinant mouse MT with respect to Cu(I). The analysis of the results requires a progressive approach.

First, assuming an independent domain behaviour [11], the stoichiometry of the species found in the titrations of the α and β fragments allows us to infer possible metal distributions between domains for the copper and copper-zinc species obtained in the titrations of the entire MT (Table 3). The next step consists of matching the CD spectral data of the independent fragments with those of the entire MT. Among all the possible sums proposed in Table 3, the unique cases in which the structure of each domain in the entire MT is very close to that of the independent fragments are those shown in Fig. 8. Interestingly, this occurs in only 3 out of the 11 possible combinations and they correspond to the three consecutive species Cu_4Zn_5-MT, Cu_7Zn_3-MT and $Cu_{10}Zn_1$-MT formed in the pathway which leads from Zn_7-MT to Cu_{12}-MT. Conversely, we do not have experimental evidence to support a specific metal distribution between domains in any of the homometallic Cu-MT species, which form along the titrations at both pH values. Before we deal with these observations, it is of interest to take into account additional findings.

On the one hand, it is widely accepted that a Cu_{12}-MT species in mammalian MT consists of a $(Cu_6)^{\alpha}(Cu_6)^{\beta}$–MT metal distribution [8, 18]. However, despite our many attempts to identify a Cu_6-αMT form neither spectral data nor the ESI-MS measurements are consistent with its presence in solution at pH 3 or 7. Accordingly, on the basis of the proposed independent behaviour of the α and β domains [11], we cannot support a $(Cu_6)^{\alpha}(Cu_6)^{\beta}$–MT metal distribution for Cu_{12}-MT at these pH values. A parallel question is raised by the Cu_6-MT and Cu_9-MT species at pH 3. In agreement with the general belief, if Cu(I) had a preferential binding for the β domain it would be reasonable to consider the $(apo)^{\alpha}(Cu_6)^{\beta}$–MT and $(Cu_3)^{\alpha}(Cu_6)^{\beta}$–MT distributions for these species, respectively. However, our spectral data indicate that the previous metal distributions cannot be assigned to the Cu_6-MT and Cu_9-MT species. Even though the similarity of the shapes of the CD spectra of Cu_6-MT and Cu_9-MT with that of Cu_6-βMT (Fig. 9) would be in favour of the co-ordination of Cu(I) to the β fragment, the UV-Vis difference spectra of the first stages of the titration of apo-MT with Cu(I), which resemble those of apo-αMT, would agree with Cu(I) also binding to the α domain in the entire MT. All these results indicate that in the Cu_6-MT, Cu_9-MT and Cu_{12}-MT species there is no evidence for the presence of an independent Cu_6-βMT domain. Instead, in the case of Cu_6-MT and Cu_9-MT it seems that Cu(I) ions distribute between both the α and β domains, as previously pointed out by Li & Weser [8]. Distribution of Cu in the two domains also happens in the mixed-metal MT species obtained at pH 7. The addition of Cu(I) to Cu_4Zn_5-MT $[(Zn_4)^{\alpha}(Cu_4Zn_1)^{\beta}$–MT] causes a partial replacement of the Zn(II) ions bound to the α domain without introducing changes in the stoichiometry and structure of the β domain, and affords a Cu_7Zn_3-MT $[(Cu_3Zn_2)^{\alpha}(Cu_4Zn_1)^{\beta}$–MT] species. The remaining Zn(II) ion bound to the N-terminal β domain is not replaced until 10 Cu(I) equivalents have been added to Zn_7-MT, which renders a $Cu_{10}Zn_1$-MT $[(Cu_4Zn_1)^{\alpha}(Cu_6)^{\beta}$–MT] species. Unlike the Cu_6-MT, Cu_9-MT and Cu_{12}-MT species, the $Cu_{10}Zn_1$-MT species is the only one in which there is evidence of the existence of a Cu_6-βMT cluster.

One of the methods commonly used to obtain Cu_6-βMT from mammalian MT consists of recovering apo-MT from the native MT, then addition of 6 Cu(I) per mol and finally digestion with subtilisin [38]. According to our results the addition of 6 Cu(I) to the apoform of recombinant mouse MT yields a Cu_6-MT species with Cu(I) distributed among both domains. This could explain why the previous procedure has not been adequate for obtaining homogeneous and well-structured samples. It seems that a good method to achieve the recovery of pure Cu_6-βMT could be the expression of the β fragment in zinc-supplemented media and then replacement of Zn by Cu either at acidic or neutral pH [24].

Overall, it seems that the presence of Zn(II) in the α domain is essential to maintain the structure of Cu-MT species in two domains. In cases where only Cu(I) but not Zn(II) is bound to MT, which occurs all along the titration at pH 3 or by addition of at least 12 Cu(I) ions to Zn_7-MT at pH 7, the folding of the protein is probably best described as a unique MT domain rather than the characteristic bi-dominial structure. Furthermore, our data strongly suggest that species formed at different pH values but with the same Cu(I)/MT ratio (Cu_7-αMT, Cu_9-αMT, Cu_{12}-MT, Cu_{15}-MT) do not have the same structure. Thus, the final folding of the Cu-MT species seems to be determined by the reaction pathway followed for their formation. At pH 7, but not at pH 3, Zn(II) ions are co-ordinated to the protein and thus they are responsible for a template effect, pre-conditioning the structure of the protein before they are replaced by Cu(I). Nevertheless, the strong affinity of Cu(I) for cysteine thiolates explains the significant degree of folding of Cu-MT species in the absence of Zn(II).

In order to investigate the presence of Zn(II) as a keystone also in the structure of the *in vivo*-conformed mouse Cu-MT, we undertook the recombinant synthesis of the α fragment and the entire protein by bacteria grown in Cu-supplemented media. Using the same conditions as those for the β fragment, which lead to a mixture of 25% Cu_6-βMT and 75% Cu_7-βMT homometallic species [1], the expression of the α fragment rendered a mixture of Cu_4Zn_1-αMT, Cu_5Zn_1-αMT and Cu_7-αMT, Fig. 7B-C and Table 2. That of the entire MT afforded a unique Cu_7Zn_3-MT species (Table 2),

which according to CD data (Fig. 7A) has a $(Cu_3Zn_2)^{\alpha}(Cu_4Zn_1)^{\beta}$–MT metal distribution. Overall, the stoichiometries of the metal aggregates obtained *in vivo* reveal that while the expression of MT and the α fragment affords Cu,Zn mixed-metal species, the β fragment contains Cu(I) ions exclusively. The stoichiometry and structure of the metal aggregates formed in all the *in vivo* synthesis are consistent with those obtained in the *in vitro* experiments at pH 7 and are in concordance with the common belief that Zn(II) unlike Cu(I) prefers to be bound to the α than to the β fragment [10-12]. However these preferences should be considered only as a general tendency and not as an absolute rule, as during the titration of Zn_7-MT with Cu(I) at neutral pH, the first 4 Cu(I) ions bind to the β domain, the next 3 to the α domain and the following 3 to both domains, eventually affording a $(Cu_4Zn_1)^{\alpha}(Cu_6)^{\beta}$–MT species (Fig. 6).

Sound evidence supports that the stable *in vivo*-conformed Cu-thionein for mouse MT is not a fully Cu-loaded MT, but a unique Cu,Zn mixed-metal species (Cu_7Zn_3-MT). This includes one zinc atom in the β domain and two in the α domain, the latter being essential for maintaining its structure in two separate metal clusters. Cu_7Zn_3-MT, one of the intermediate species obtained *in vitro* in the Zn/Cu replacement pathway, should represent the most stable Cu,Zn cluster in physiological conditions. Therefore, our results agree with the hypothesis that MT is currently synthesised in the cell as a Zn-complex, from which some zinc ions are replaced in the presence of high concentrations of other metals, forming mixed-metal clusters stabilised by the permanence of Zn. This agrees with the fact that the native MT obtained from Cd- [4, 8, 30] or from Cu- [25-29] treated animals is always a mixed-metal cluster including some Zn atoms, and also with the old observation that Cu-MT produced after Cu treatment by Zn-depleted rats exhibited a shorter biological life than the same molecules produced by Zn-supplemented animals [26]. The reason why no homometallic mammal Cu-MT species are formed *in vivo* can be related to the potential functions of the MT protein. According to our data, the presence of Zn promotes and maintains the folding of MT into two domains, even after partial Zn/Cu replacement. The bi-dominial structure of MT has been claimed as being very important for its interaction with ligands and for

control of its reactivity [33]. On the other hand, it has been shown by NMR analysis of the yeast MT protein part that a variety of cluster arrangements are possible for the seven Cu ions bound [39]. This, together with the inability of Cu alone to determine a bi-dominial MT molecule under physiological conditions, would be incompatible with a unique MT structure associated to a definite biological role. The previous considerations allow a further extension. Thus, it is tempting to propose that the release of Zn(II) accompanying formation of Cu_7Zn_1-MT may be related to recent findings on the regulation of mammalian MT synthesis in front of abnormally high concentrations of metals other than Zn. It has been reported that the DNA binding ability of MTF-1 is only Zn-activated [32]. Then, it is likely that the ability for other metals to enhance MT synthesis relies on Zn/metal MT replacement processes in original Zn-MT molecules, and that the released Zn ions become the triggering mechanism for MT gene transcription via MTF-1 activation.

The existence of domain interactions in the entire MT protein have already been proposed for other mammalian MT species [21, 33], and is now corroborated by our data on mammalian Cu-MT. When independently expressed, the β domain renders a mixture of Cu_6-βMT and Cu_7-βMT species and the α domain a mixture of Cu_4Zn_1-αMT, Cu_5Zn_1-αMT and Cu_7-αMT. Instead, the entire MT yields a unique Cu_7Zn_1-MT species, with a $(Cu_4Zn_1)^{\beta}(Cu_3Zn_2)^{\alpha}$-MT metal distribution. If comparing the Cu(I) content of each domain in this species with that of the independently expressed α and β domains, a loss of Cu co-ordination capacity *in vivo* can be observed when both domains are part of a unique protein structure. Presumably, this could be attributed to the amino acids of the central peptide fragment involved in domain bridging, which cannot contribute to the formation of metal clusters stable in the cellular conditions. Thus, a bi-dominial MT structure is not concomitant with an absolute independent behaviour for each domain.

The involvement of zinc in other metalloproteins classically defined as copper-species is being revealed nowadays by means of recombinant synthesis and highly sensitive spectroscopic and spectrometric techniques. Particularly significant is the case of the yeast transcription factors for MT genes, ACE1 and AMT1, whose

Cu-responsive domain had been previously described as a 6-7 Cu cluster, and has now been characterised as a Cu_4Zn_1 mixed-metal cluster, which may result from metal replacement in a pre-existent silent Zn form [40, 41]. Mammalian copper-thioneins would be, according to our results, a striking new example of this phenomenon, and consequently, efforts seek their biological role would be better centred upon the Cu_7Zn_3-MT species than on the *in vitro*-folded forms. Even more, a full examination of the data reported in the literature for *in vivo* Cu-MT lead to the conjecture that in fact all these proteins result from a Zn/Cu replacement in original Zn-containing forms. This process of substitution would be complete in the so-called copper-thioneins while being only partial in more evolved MT. It is worth noting that the metal analysis of the recombinant yeast CUP1 synthesised by Cu-supplemented bacteria yielded an unexpected content of 1 Zn/mol [42], and that the stoichiometry for the native copper-specific *Helix pomatia* MT has been reported as 100:6 for Cu:Zn [43].

At this stage, evolutionary implications for the different behaviour of the β-type and α-type MT domains in copper cluster formation can be drawn. All well defined β-type MT mainly result in homometallic Cu-containing species when expressed by recombinant techniques: yeast CUP1 [42], *Drosophila* MTN [44] and the independent mammalian β domain [1]. On the other hand, in the bi-dominial MT which contain α domains, evolution to optimise divalent metal chelation would have supposed a concomitant loss of capacity to fully exchange Zn by Cu ions *in vivo* and, therefore, would never render homometallic Cu-MT species when synthesised in Cu-enriched cellular environments.

Acknowledgements This work was supported by the projects PB97-0216 and PN96-0225 from the Spanish Ministerio de Educación y Cultura, and the UE contract BIO4-CT97-2123. R.B. is indebted to the Comissionat per a Universitats i Recerca de la Generalitat de Catalunya (CIRIT) for a pre-doctoral scholarship. We acknowledge the Servei d'Anàlisi Química, Universitat Autònoma de Barcelona (AAS, CD, UV-Vis), the Serveis Científico-Tècnics, Universitat de Barcelona (ICP-AES, ESI-MS) and the ICMAB (EPR) for allocating instrument time.

References

1. Cols N, Romero-Isart N, Bofill R, Capdevila M, Gonzàlez-Duarte P, Gonzàlez-Duarte R, Atrian S (1999) Protein Eng 12: 265-269
2. Suzuki KT, Imura N, Kimura M (eds) (1993) Metallothionein III. Birkhäuser Verlag, Basel
3. Klaassen CD (ed) (1999) Metallothionein IV. Birkhäuser Verlag, Basel
4. Robbins AH, McRee DE, Williamson M, Collett SA, Xuong NH, Furey WF, Wang BC, Stout CD (1991) J Mol Biol 221: 1269-1293
5. Kull FJ, Reed MF, Elgren TE, Ciardelly TL, Wilcox DE (1990) J Am Chem Soc 112: 2291-2298
6. Li Y, Zhang L, Bayer E, Oelkrug D, Weser U (1990) Z Naturforsch C 45: 1193-1196
7. Hartmann HJ, Li YJ, Weser U (1992) BioMetals 5: 187-191
8. Li Y, Weser U (1992) Inorg Chem 31: 5526-5533
9. Kurasaki M, Yamasaki F, Suzuki-Kurasaki M, Kojima Y (1996) Res Commun Mol Pathol Pharmacol 92: 225-232
10. Nielson KB, Winge DR (1984) J Biol Chem 259: 4941-4946
11. Nielson KB, Winge DR (1985) J Biol Chem 260: 8698-8701
12. Chen P, Muñoz A, Nettesheim D, Shaw III CF, Petering DH (1996) Biochem J 317: 395-402
13. Pountney DL, Schauwecker I, Zarn J, Vašák M (1994) Biochemistry 33: 9699-9705
14. Green AR, Stillman MJ (1994) Inorg Chim Acta 226: 275-283
15. Presta A, Green AR, Zelazowski A, Stillman MJ (1995) Eur J Biochem 227: 226-240
16. Green AR, Stillman MJ (1996) Inorg Chem, 35: 2799-2807
17. Geller BL, Winge DR (1982) Arch Biochem Biophys 213: 109-117
18. Li H, Otvos JD (1996) Biochemistry 35: 13929-13936
19. Jensen LT, Peltier JM, Winge DR (1998) JBIC 3: 627-631
20. Palmiter RD (1998) Proc Natl Acad Sci USA 95: 8428-8430
21. Cols N, Romero-Isart N, Capdevila M, Oliva B, Gonzàlez-Duarte P, González-Duarte R, Atrian S (1997) J Inorg Biochem 68: 157-166

22. Capdevila M, Cols N, Romero-Isart N, Gonzàlez-Duarte R, Atrian S, González-Duarte P (1997) Cell Mol Life Sci 53: 681-688
23. Atrian S, Bofill R, Capdevila M, Cols N, Gonzàlez-Duarte P, Gonzàlez-Duarte R, Leiva A, Palacios O, Romero-Isart N (1999) In: Klaassen CD (ed) Metallothionein IV. Birkhäuser Verlag, Basel, pp 55-61
24. Bofill R, Palacios O, Capdevila M, Cols N, Gonzàlez-Duarte R, Atrian S, Gonzàlez-Duarte P (1998) J Inorg Biochem 73: 57-64
25. Bremner I, Young B (1976) Biochem J 155: 631-635
26. Bremner I, Young B (1976) Biochem J 157: 517-520
27. Briggs RW, Armitage IM (1982) J Biol Chem 257: 1259-1262
28. Abrahams IL, Bremner I, Diakun GP, Garner CD, Hasnain SS, Ross I, Vašák M (1986) Biochem J 236: 585-589
29. Chen P, Onana P, Shaw III CF, Petering DH (1996) Biochem J 317: 389-394
30. Otvos JD, Armitage IM (1980) Proc Natl Acad Sci USA 77: 7094-7098
31. Uversky VN, Gillespie JR, Millett IS, Khodyakova AV, Vasilenko RN, Vasiliev AM, Rodionov IL, Kozlovskaya GD, Dolgikh DA, Fink AL, Doniach S, Permyakov EA, Abramov VM (2000) Biochem Biophys Res Commun 267: 663-668
32. Bittel D, Dalton T, Samson SLA, Gedamu L, Andrews GK (1998) J Biol Chem 273: 7127-7133
33. Jiang LJ, Vašák M, Vallee BL, Maret W (2000) Proc Natl Acad Sci USA 97: 2503-2508
34. Kubas GJ (1979) Inorg Synth 19: 90-92
35. Bongers J, Walton CD, Richardson DE, Bell JU (1988) Anal Chem 60: 2683-2686
36. Fabris D, Zaia J, Hathout Y, Fenselau C (1996) J Am Chem Soc 118: 12242-12243
37. Zaia J, Fabris D, Wei D, Karpel RL, Fenselau C (1998) Protein Sci 7: 2398-2404
38. Winge DR (1991) Methods Enzymol 205: 438-447
39. Bertini I, Hartmann, HJ, Klein T, Liu G, Luchinat C, Weser U (2000) Eur J Biochem 267: 1008-1018
40. Dameron CT, Winge DR, George GN, Sansone M, Hu S, Hamer D (1991) Proc Natl Acad Sci USA 88: 6127-6131

41. Thorvaldsen JL, Sewell AK, Tanner AM, Peltier JM, Pickering IJ, George GN, Winge DR (1994) Biochemistry 33: 9566-9577
42. Sayers Z, Brouillon P, Vorgias CE, Nolting HF, Hermes C, Koch MHJ (1993) Eur J Biochem 212: 512-528
43. Berger B, Dallinger R, Gehrig P, Hunziker PE (1997) Biochem J 328: 219-224
44. Valls M, Bofill R, Romero-Isart N, Gonzàlez-Duarte R, Abián J, Carrascal M, Gonzàlez-Duarte P, Capdevila M, Atrian S (2000) FEBS Lett 467: 189-194

Table 1. Molecular masses found for the Cu,Zn-MT mixed-metal species obtained during the titrations of Zn_4-αMT and Zn_7-MT with Cu(I) at pH 7 and molecular masses found for the Cu-MT species obtained during the titration of apo-MT with Cu(I) at pH 3.

Titrated species	Cu(I) equivalents added	Experimental molecular masses	MT species (calculated molecular masses)[a]
Zn_4-αMT	2	3550.97 ± 0.57	Zn_4-αMT (3550.45)
		3609.88 ± 1.63	Cu_3Zn_2-αMT (3611.33)
	3	3611.31 ± 1.22	Cu_3Zn_2-αMT (3611.33)
	4	3609.21 ± 1.30	Cu_4Zn_1-αMT (3610.49)
	5	3672.38 ± 1.61	Cu_5Zn_1-αMT (3673.04)
Apo-MT	3	6159.35 ± 2.51	apo-MT (6162.13)
		6536.57 ± 5.75	Cu_6-MT (6537.41)
	6	6532.10 ± 5.95	Cu_6-MT (6537.41)
Zn_7-MT	4	6731.04 ± 4.50	Cu_4Zn_5-MT (6729.26)
	6	6728.35 ± 9.15	Cu_4Zn_5-MT (6729.26)
		6794.70 ± 10.80	Cu_7Zn_3-MT (6790.09)
	7	6788.50 ± 8.88	Cu_7Zn_3-MT (6790.09)
	9	6787.20 ± 2.20	Cu_7Zn_3-MT (6790.09)
		6854.66 ± 9.53	$Cu_{10}Zn_1$-MT (6850.97)
	10	6852.35 ± 7.15	$Cu_{10}Zn_1$-MT (6850.97)
	12	6909.06 ± 10.07	Cu_{12}-MT (6912.68)
	15	7098.8 ± 1.52	Cu_{15}-MT (7100.32)

[a]Calculated masses for neutral species with loss of two protons per zinc bound and one proton per copper bound [36].

Table 2. Molecular masses and zinc and copper per protein molar ratio found for *in vivo*-synthesized Cu-MT and Cu-αMT species.

Protein expressed in Cu-supplemented media	m (holoprotein)[a]	(Zn/protein)[b]	(Cu/protein)[b]
MT	6790.08 ± 0.21	2.4	7.2
αMT	3607.85 ± 2.85 (M) 3676.47 ± 1.95 (m)	0.5	4.5

[a]Determined molecular masses of the Cu,Zn-protein complexes. (M) denotes major and (m) minor species. Calculated masses for neutral species with loss of two protons per zinc bound and one proton per copper bound [36] are 6790.09 (Cu_7Zn_3-MT), 3610.49 (Cu_4Zn_1-αMT) and 3673.04 (Cu_5Zn_1-αMT).

[b]Zinc and copper per protein molar ratio calculated from the content of zinc, copper and total sulfur (ICP-AES) [22].

Table 3. Possible metal distributions between domains in recombinant entire mouse Cu-MT based on the stoichiometries found for the independent fragments. The metal distributions that have been deduced from experimental data are depicted in bold.

Stoichiometry of the MT species at pH 3	Possible metal distributions	Stoichiometry of the MT species at pH 7	Possible metal distributions
Cu_6-MT	$(apo)^{\alpha}(Cu_6)^{\beta}$-*MT*	Cu_4Zn_5-MT	$\mathbf{(Zn_4)^{\alpha}(Cu_4Zn_1)^{\beta}}$**-MT**
Cu_9-MT	$(Cu_3)^{\alpha}(Cu_6)^{\beta}$-*MT* $(Cu_9)^{\alpha}(apo)^{\beta}$-*MT*	Cu_7Zn_3-MT	$\mathbf{(Cu_3Zn_2)^{\alpha}(Cu_4Zn_1)^{\beta}}$**-MT**
Cu_{11}-MT	$(Cu_5)^{\alpha}(Cu_6)^{\beta}$-*MT*	$Cu_{10}Zn_1$-MT	$\mathbf{(Cu_4Zn_1)^{\alpha}(Cu_6)^{\beta}}$**-MT**
Cu_{12}-MT	$(Cu_5)^{\alpha}(Cu_7)^{\beta}$-*MT*		
Cu_{15}-MT	$(Cu_9)^{\alpha}(Cu_6)^{\beta}$-*MT* $(Cu_5)^{\alpha}(Cu_{10})^{\beta}$-*MT*	Cu_{15}-MT	$(Cu_9)^{\alpha}(Cu_6)^{\beta}$-*MT*

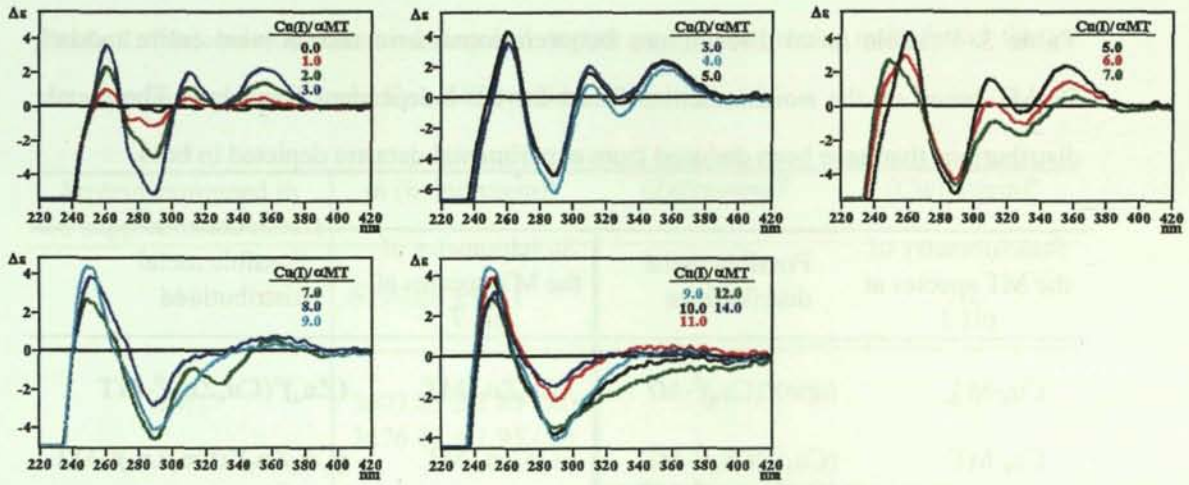

Figure 1.- CD spectra corresponding to the Cu(I) titration of a $2.00 \cdot 10^{-5}$ M solution of recombinant apo-αMT at pH 3. The Cu(I) to MT molar ratios are indicated within each frame.

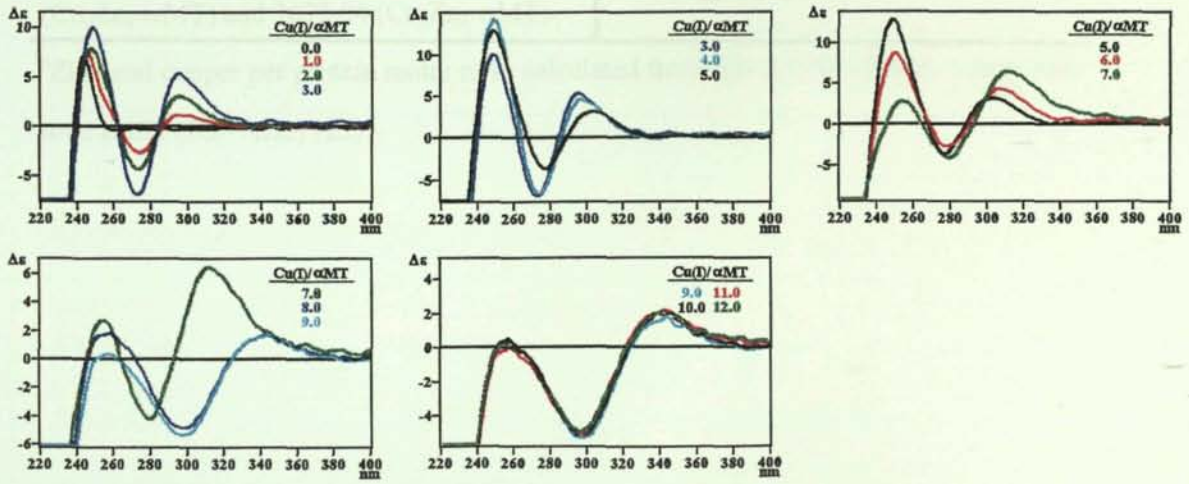

Figure 2.- CD spectra corresponding to the Cu(I) titration of a $2.00 \cdot 10^{-5}$ M solution of recombinant Zn_4-αMT at pH 7. The Cu(I) to MT molar ratios are indicated within each frame.

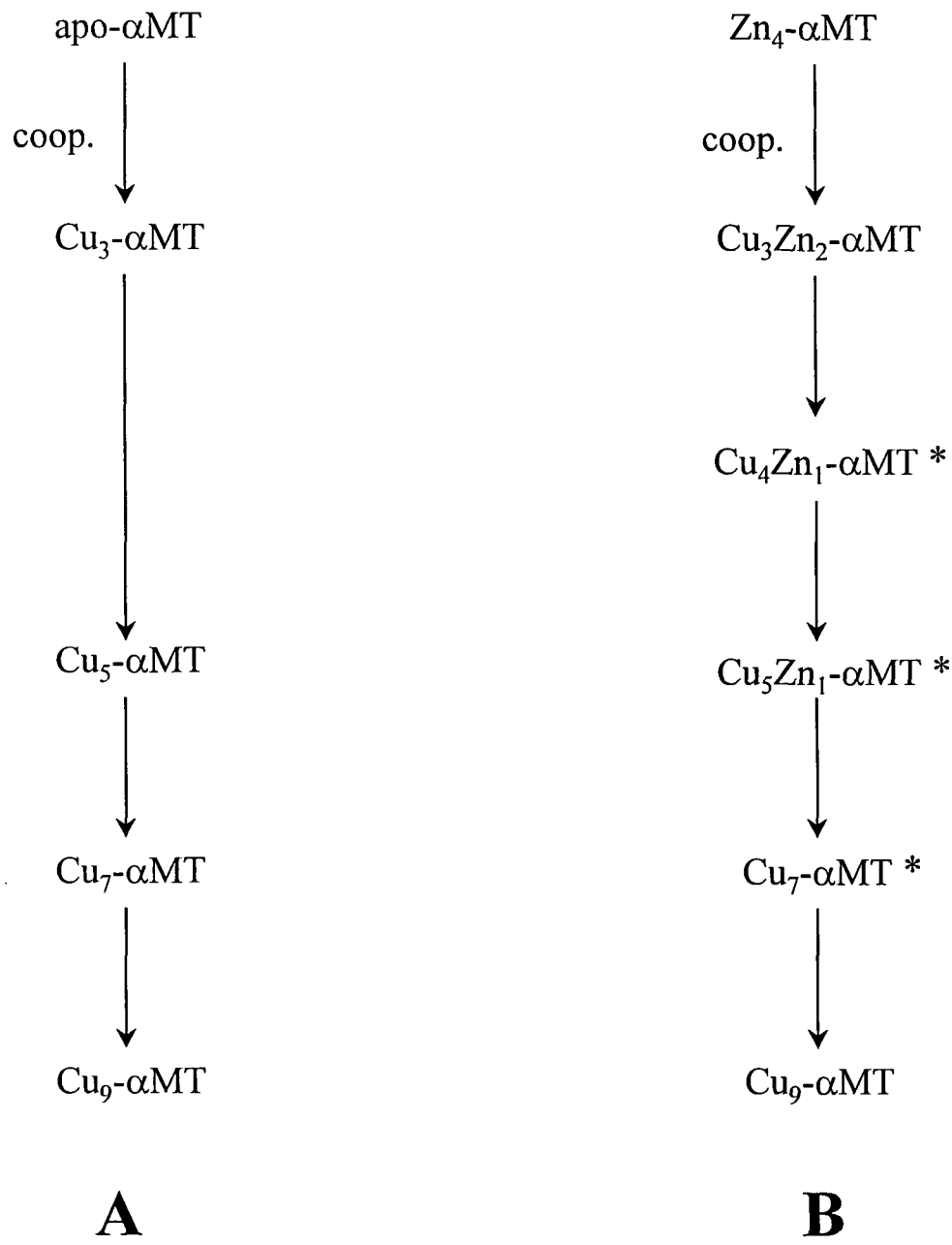

Figure 3.- Proposed reaction pathways for Cu(I) binding to recombinant apo-αMT at pH 3 (A) and recombinant Zn_4-αMT at pH 7 (B). MT species recovered from recombinant synthesis in Cu-supplemented media are denoted by *.

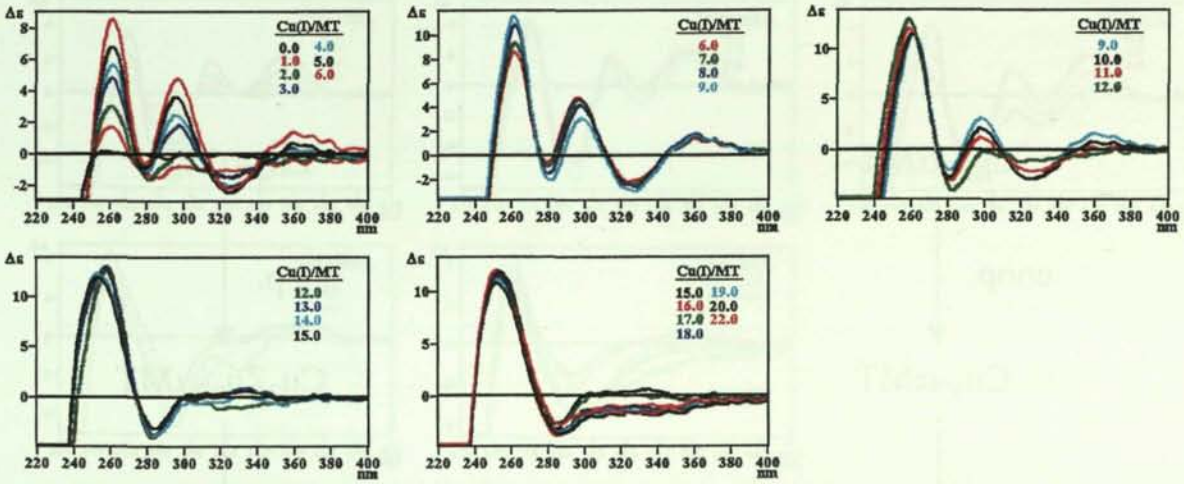

Figure 4.- CD spectra corresponding to the Cu(I) titration of a $1.00 \cdot 10^{-5}$ M solution of recombinant apo-MT at pH 3. The Cu(I) to MT molar ratios are indicated within each frame.

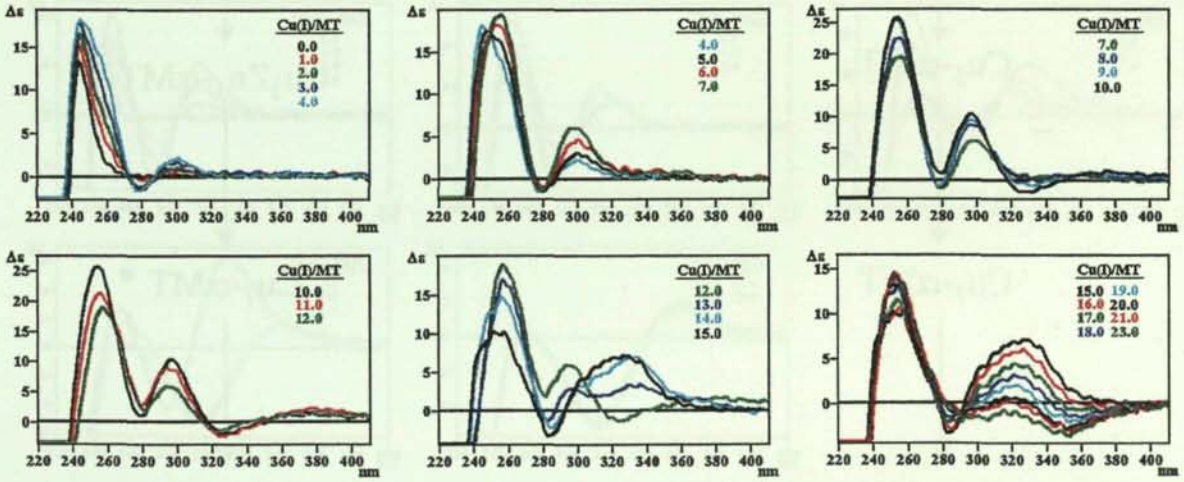

Figure 5.- CD spectra corresponding to the Cu(I) titration of a $9.99 \cdot 10^{-6}$ M solution of recombinant Zn_7-MT at pH 7. The Cu(I) to MT molar ratios are indicated within each frame.

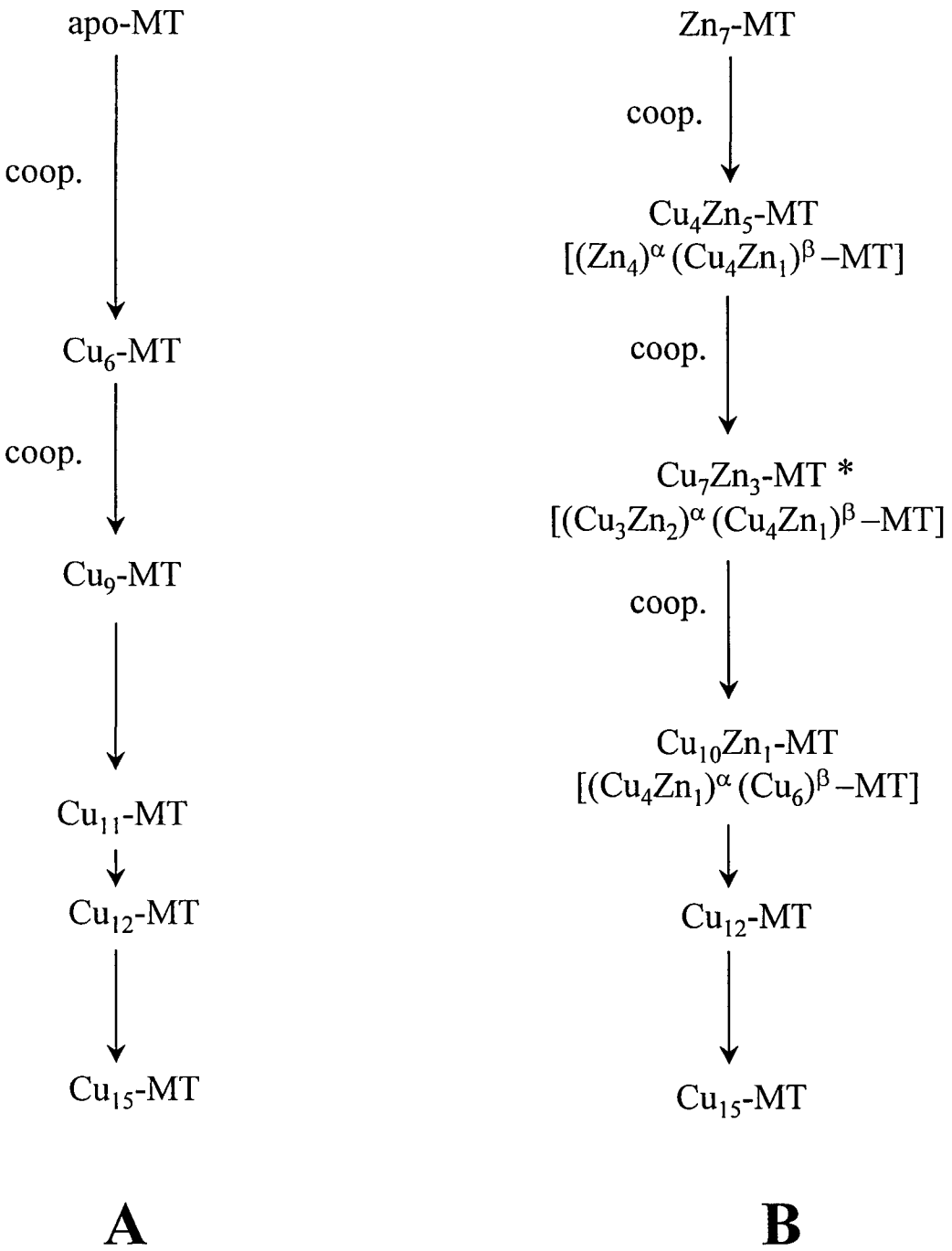

Figure 6.- Proposed reaction pathways for Cu(I) binding to recombinant apo-MT at pH 3 (A) and recombinant Zn_7-MT at pH 7 (B). The metal distribution between domains proposed for the mixed-metal species will be discussed below. MT species recovered from recombinant synthesis in Cu-supplemented media are denoted by *.

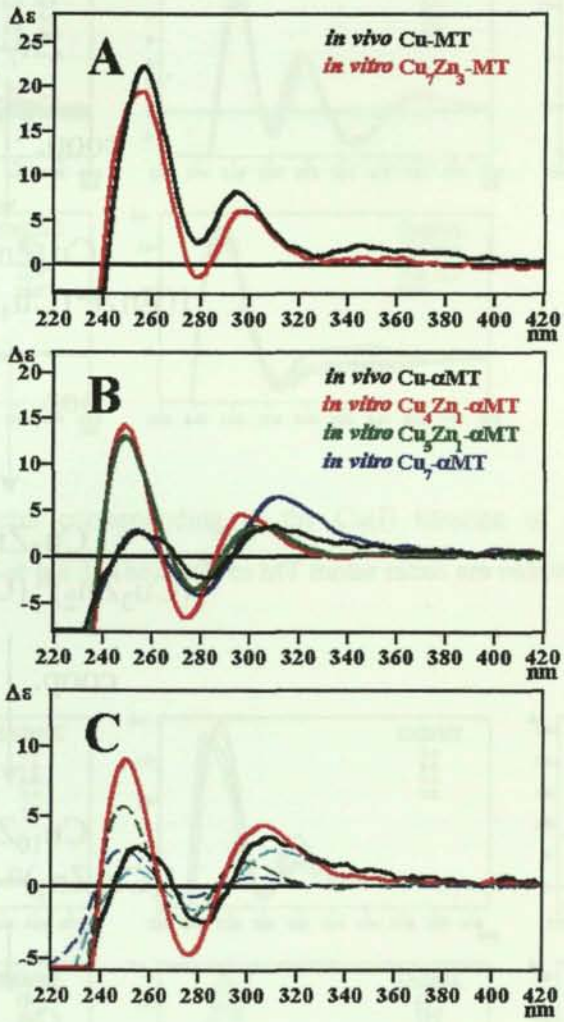

Figure 7.- Comparison of the circular dichroism spectra of the *in vivo*-synthesised Cu-MT (A) and Cu-αMT (B) species with those corresponding to the *in vitro* Cu_7Zn_3-MT (A) and Cu_4Zn_1-αMT, Cu_5Zn_1-αMT and Cu_7-αMT species (B). In Figure 7C a computer generated spectrum (in red) corresponding to the sum of the circular dichroism spectral traces (in dashed lines) of Cu_4Zn_1-αMT (40%, in green), Cu_5Zn_1-αMT (20%, in blue) and Cu_7-αMT (40%, in turquoise) is compared to the CD spectra corresponding to the *in vivo*-synthesised Cu-αMT species (in black).

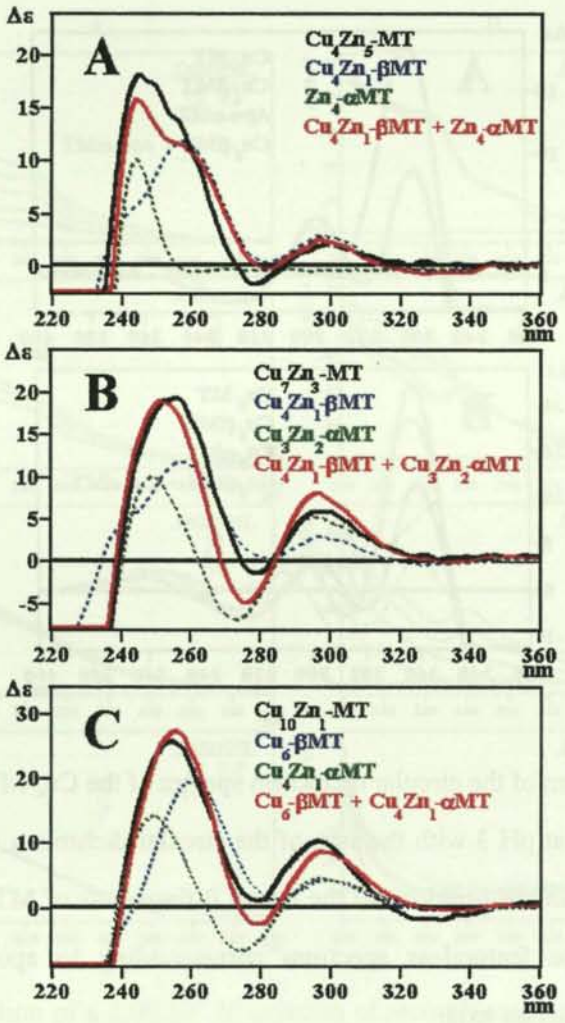

Figure 8.- Comparison of the circular dichroism spectra of the Cu,Zn mixed-metal species formed during the titration of Zn_7-MT at pH 7 with Cu(I) [(A) Cu_4Zn_5-MT, (B) Cu_7Zn_3-MT, (C) $Cu_{10}Zn_1$-MT] with the sum of the circular dichroism spectra of some of the species obtained in the titrations of the α and β fragments of MT with Cu(I) at the same pH value.

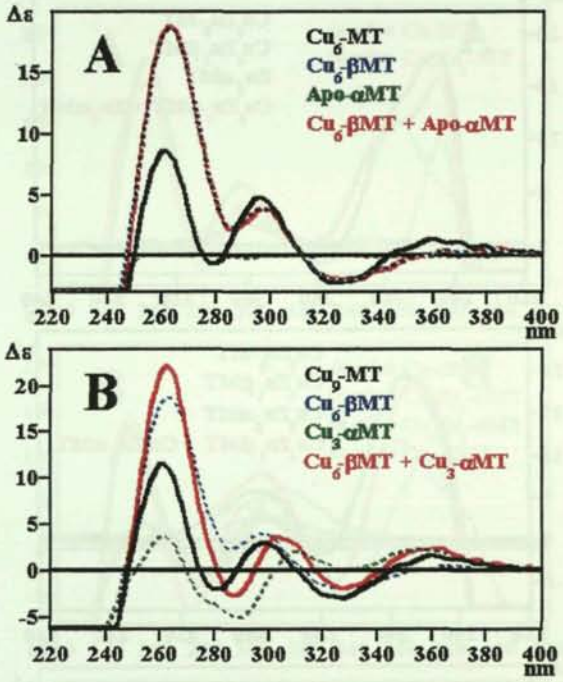

Figure 9.- Comparison of the circular dichroism spectra of the Cu_6-MT (A) and Cu_9-MT (B) species obtained at pH 3 with the sum of the circular dichroism spectra of some of the species obtained in the titrations of the α and β fragments of MT with Cu(I) at the same pH value. The featureless spectrum corresponding to apo-αMT practically coincides with the abscissa axis.

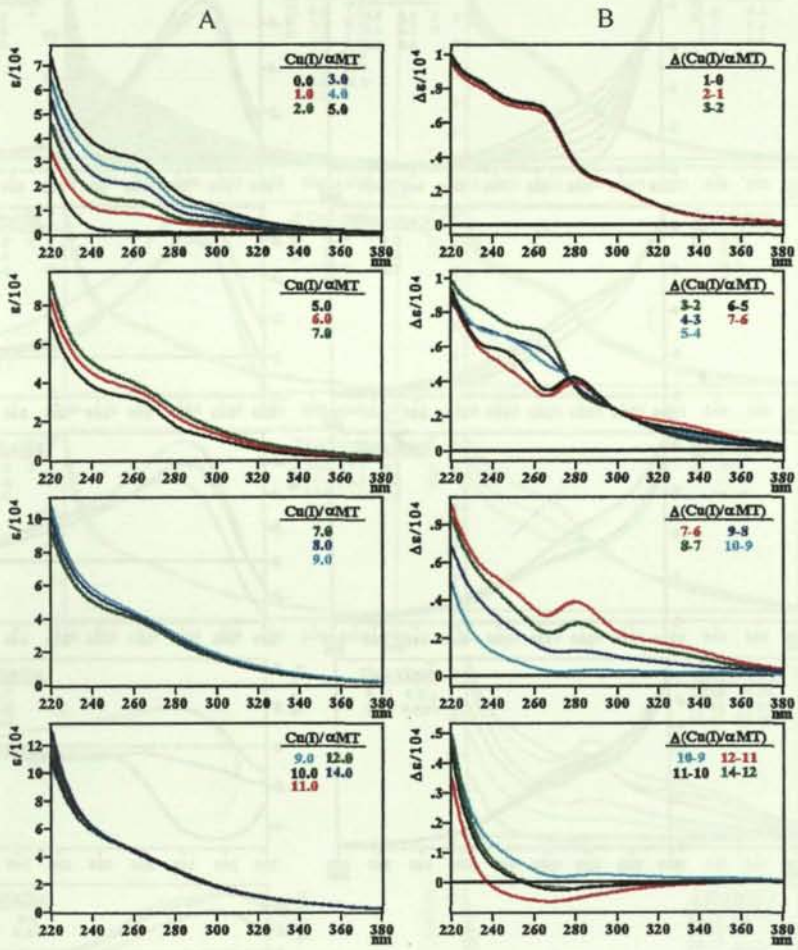

Figure S1.- Cu(I) titration of a $2.00 \cdot 10^{-5}$ M solution of recombinant apo-αMT at pH 3. (A) UV-Vis absorption spectra. (B) Difference absorption spectra obtained by subtracting the successive spectra of (A). For the sake of comparison, their intensities have been normalised with respect to one molar addition. The Cu(I) to MT molar ratios are indicated within each frame.

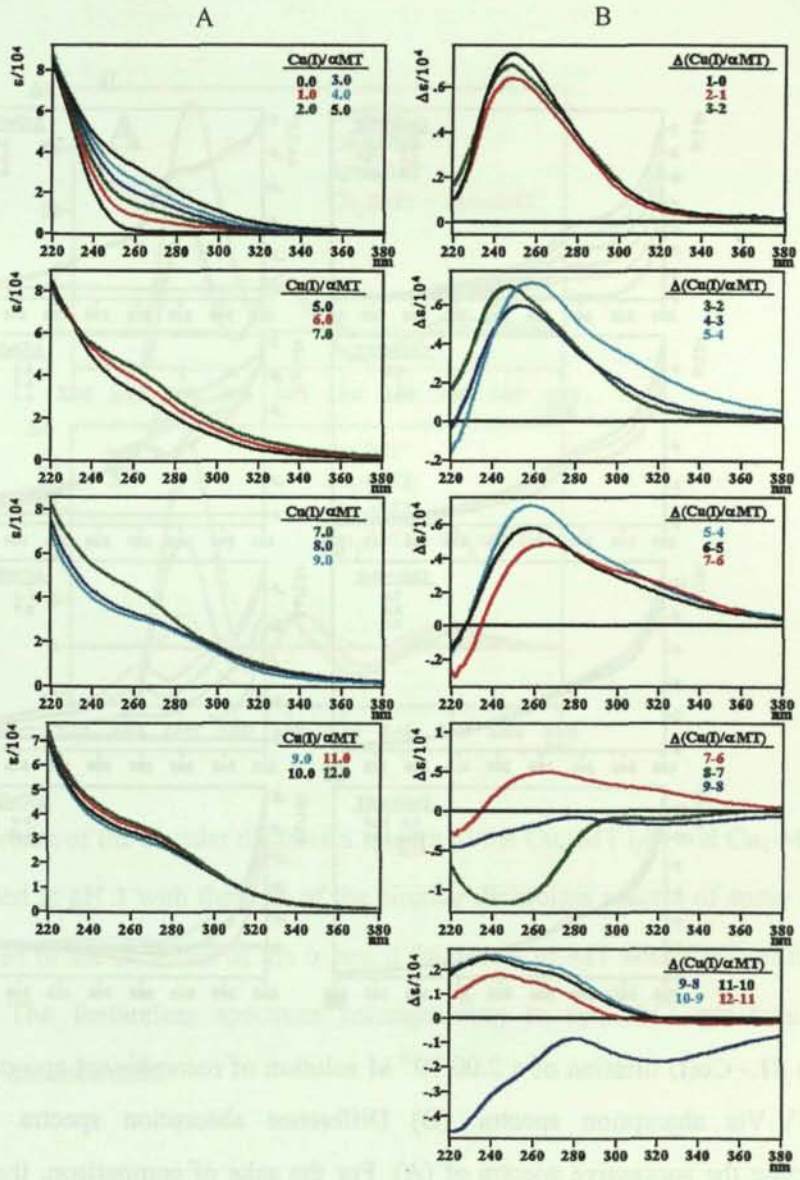

Figure S2.- Cu(I) titration of a $2.00 \cdot 10^{-5}$ M solution of recombinant Zn_4-αMT at pH 7. (A) UV-Vis absorption spectra. (B) Difference absorption spectra obtained by subtracting the successive spectra of (A). For the sake of comparison, their intensities have been normalised with respect to one molar addition. The Cu(I) to MT molar ratios are indicated within each frame.

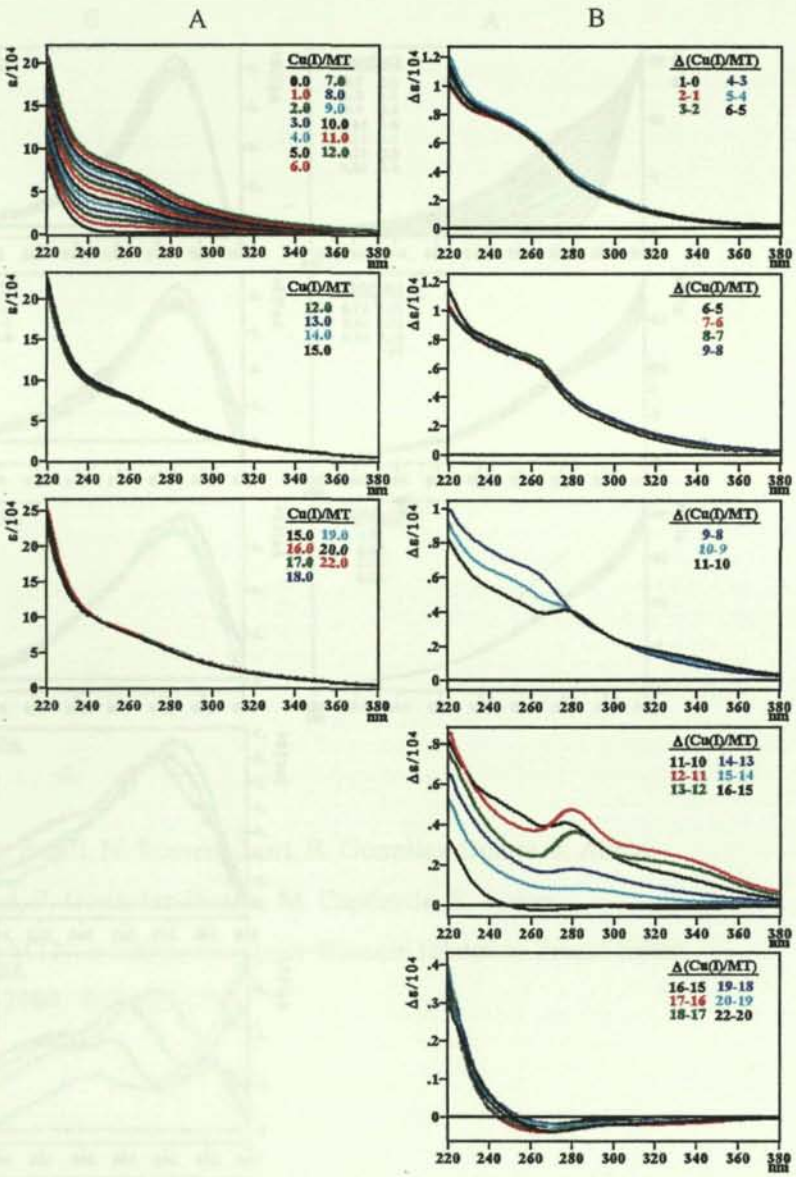

Figure S3.- Cu(I) titration of a $1.00 \cdot 10^{-5}$ M solution of recombinant apo-MT at pH 3. (A) UV-Vis absorption spectra. (B) Difference absorption spectra obtained by subtracting the successive spectra of (A). For the sake of comparison, their intensities have been normalised with respect to one molar addition. The Cu(I) to MT molar ratios are indicated within each frame.

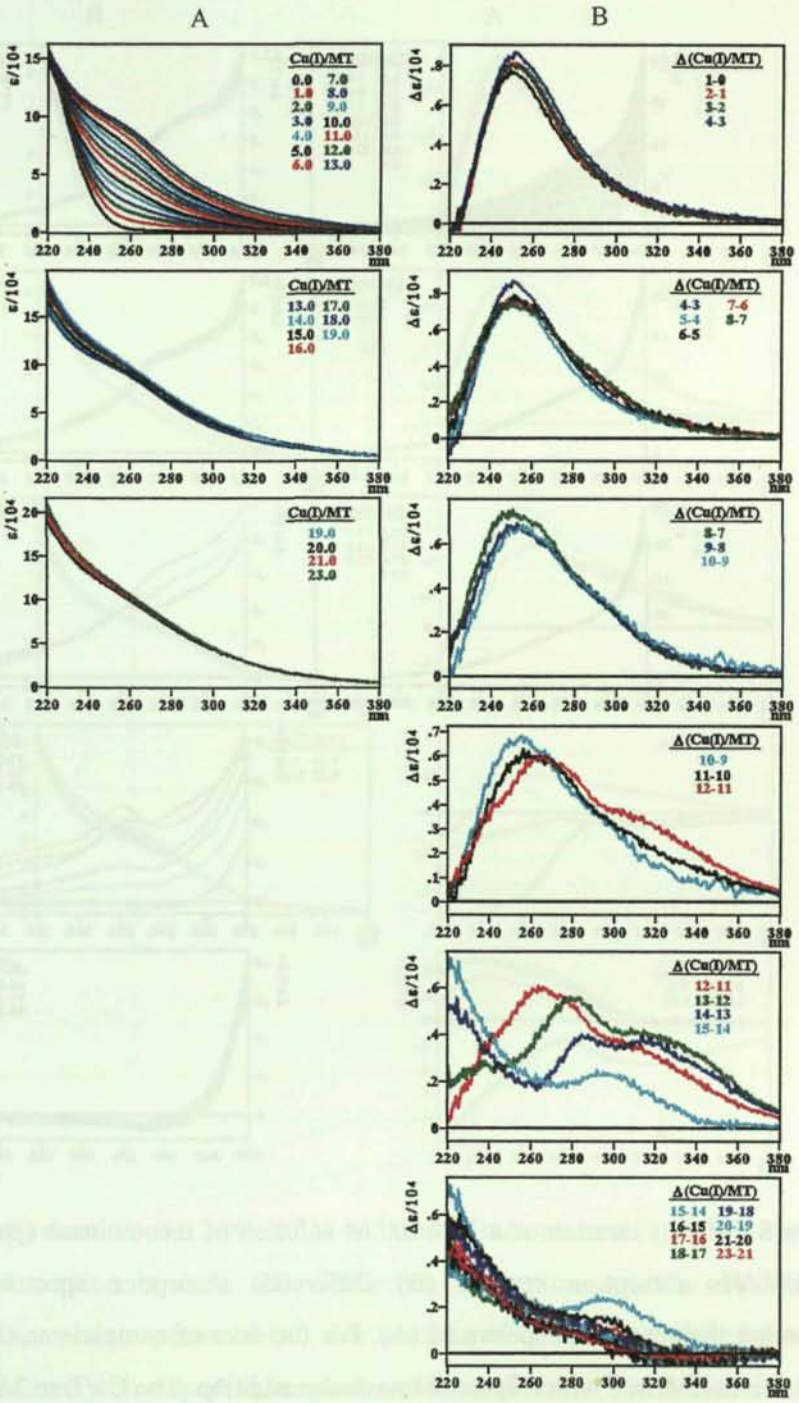

Figure S4.- Cu(I) titration of a $9.99 \cdot 10^{-6}$ M solution of recombinant Zn_7-MT at pH 7. (A) UV-Vis absorption spectra. (B) Difference absorption spectra obtained by subtracting the successive spectra of (A). For the sake of comparison, their intensities have been normalised with respect to one molar addition. The Cu(I) to MT molar ratios are indicated within each frame.